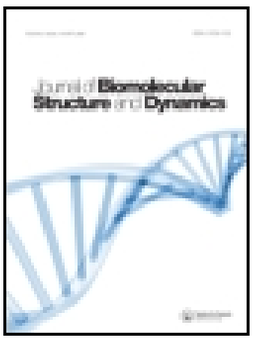

Taylor & Francis
Taylor & Francis Group

Journal of Biomolecular Structure and Dynamics

ISSN: (Print) (Online) Journal homepage: https://www.tandfonline.com/loi/tbsd20

Design and synthesis of new heterocyclic compounds containing 5-[(1*H*-1,2,4-triazol-1-yl)methyl]-3*H*-1,2,4-triazole-3-thione structure as potent hEGFR inhibitors

Yakup Kolcuoglu, Olcay Bekircan, Hilal Fazli, Emine Sahin, Aslı Ture, Atilla Akdemir & Senay Hamarat Sanlier

To cite this article: Yakup Kolcuoglu, Olcay Bekircan, Hilal Fazli, Emine Sahin, Aslı Ture, Atilla Akdemir & Senay Hamarat Sanlier (2023): Design and synthesis of new heterocyclic compounds containing 5-[(1*H*-1,2,4-triazol-1-yl)methyl]-3*H*-1,2,4-triazole-3-thione structure as potent hEGFR inhibitors, Journal of Biomolecular Structure and Dynamics, DOI: 10.1080/07391102.2023.2167113

To link to this article: https://doi.org/10.1080/07391102.2023.2167113

JOURNAL OF BIOMOLECULAR STRUCTURE AND DYNAMICS
https://doi.org/10.1080/07391102.2023.2167113

Design and synthesis of new heterocyclic compounds containing 5-[(1*H*-1,2,4-triazol-1-yl)methyl]-3*H*-1,2,4-triazole-3-thione structure as potent hEGFR inhibitors

Yakup Kolcuoglu[a], Olcay Bekircan[a], Hilal Fazli[a], Emine Sahin[a], Aslı Ture[b], Atilla Akdemir[c] and Senay Hamarat Sanlier[d,e]

[a]Department of Chemistry, Faculty of Science, Karadeniz Technical University, Trabzon, Turkey; [b]Department of Pharmaceutical Chemistry, Faculty of Pharmacy, Marmara University, Istanbul, Turkey; [c]Computer-Aided Drug Discovery Laboratory, Department of Pharmacology, Faculty of Pharmacy, Bezmialem Vakif University, Istanbul, Turkey; [d]Biochemistry Department, Faculty of Science, Ege University, Izmir, Turkey; [e]Center for Drug Research, Development and Pharmacokinetic Applications (ARGEFAR), Ege University, Izmir, Turkey

Communicated by Ramaswamy H. Sarma

ABSTRACT

EGFR is one of the important mediators of the signaling cascade that determines key roles in various biological processes such as growth, differentiation, metabolism and apoptosis in the cell in response to external and internal stimuli. In recent years, it has been proven that although this enzyme activity is tightly regulated in normal cells, if the enzyme activity cannot be controlled, it can lead to malignancy. EGFR is also considered a prominent macromolecule in targeted cancer chemotherapy. For this purpose, a comprehensive modeling studies were conducted against EGFR protein and novel molecules containing 5-[(1*H*-1,2,4-triazol-1-yl)methyl]-3*H*-1,2,4-triazole-3-thione structure were suggested to be synthesized. Among the synthesized molecules, compounds **7c**, **8c**, **8f** and **8g** were determined to have significant IC_{50} values. Compound **8g** was found to have the IC_{50} value closest to the very well-known EGFR inhibitor Gefitinib with its noncompetitive inhibition form. K_i value of compound **8g** was calculated as 0.00232 μM.

ARTICLE HISTORY
Received 22 August 2022
Accepted 6 January 2023

KEYWORDS
hEGFR; molecular modeling; docking; thiosemicarbazides; 1; 2; 4-triazoles; 1; 2; 4-triazole-3-thiones

Introduction

Cancer is the second leading cause of death in the world. Lung cancer is the most common cause of death among cancer types. Non-small cell lung cancer (NSCLC) constitutes 80% of lung cancer and consists of three main types. These are adenocarcinoma, squamous cell carcinoma and large cell carcinoma (Spira & Ettinger, 2004). Cytotoxic chemotherapy has a measurable but insufficient effect on survival. The overall survival (OS) rate is 14% as a result of treatment with state-of-the-art combined or stand-alone surgery, radiation and chemotherapy. This indicates that the response to current treatments is poor. Therefore, there is a need to develop new treatment methods and chemotherapeutic agents.

The drugs used in the traditional method do not distinguish between normal and malignant cells. Targeted therapy, on the other hand, acts by blocking essential pathways or oncoproteins required for tumor cell growth and survival. Thus, cancer cells are selectively killed compared to normal cells (Sudhakar, 2009).

Epidermal growth factor receptor (EGFR), a protein with an extracellular binding domain, a helical transmembrane domain and an intracellular tyrosine kinase domain, is the first protein discovered in the ErbB protein family (Cohen, 1962). EGFR is a protein belonging to the ErbB (avian erythroblastosis oncogene B) receptor tyrosine kinase family and is overexpressed in neoplastic cells (Bhatia et al., 2020; Normanno et al., 2003; Olayioye et al., 2000). Overexpression of EGFR in the cell has been reported to be responsible for 10–30% of NSCLC cases alone, compared to other ErbB proteins (Zhang et al., 2009). For this reason, EGFR inhibitors are currently used in the treatment of cancer. However, there are limitations in the use of existing drugs due to hypoxia-induced resistance, resistance emerging as a result of non-EGFR pathways and drug resistance (Bhatia et al., 2020).

EGFR-TKIs developed as targets in cancer treatment consist of small molecule nitrogen-containing heterocyclic compounds. However, these EGFR-TKIs used in the clinic have some undesirable disadvantages such as rash, diarrhea and loss of appetite (Ayati et al., 2020). Among the nitrogen-containing heterocyclic compounds, 1,2,4-triazoles have been of great interest to scientists due to their effective biological importance such as antibacterial (Gao et al., 2019), antifungal (Saravolatz et al., 2003), anti-inflammatory (Tariq et al., 2018), antioxidant (Khan et al., 2010), analgesic (Gajanan Khanage et al., 2013), antiviral (Kharb et al., 2011), antidiabetic (Mohamed et al., 2020), antiproliferative (Gomaa et al., 2020) and anticancer (Grytsai et al., 2020) activities. In addition, drugs containing 1,2,4-triazole core like anastrozole, letrozole

CONTACT Y. Kolcuoglu yakupkolcuoglu@yahoo.com Department of Chemistry, Faculty of Science, Karadeniz Technical University, Trabzon, 61080, Turkey.
Supplemental data for this article can be accessed online at https://doi.org/10.1080/07391102.2023.2167113.

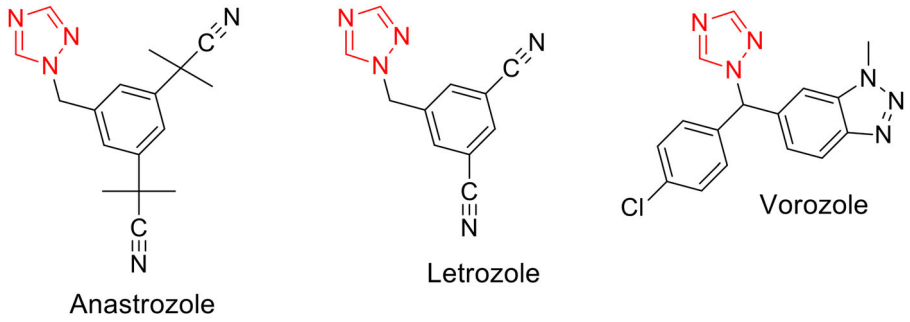

Figure 1. Some clinically used cancer drugs having 1,2,4-triazole scaffold.

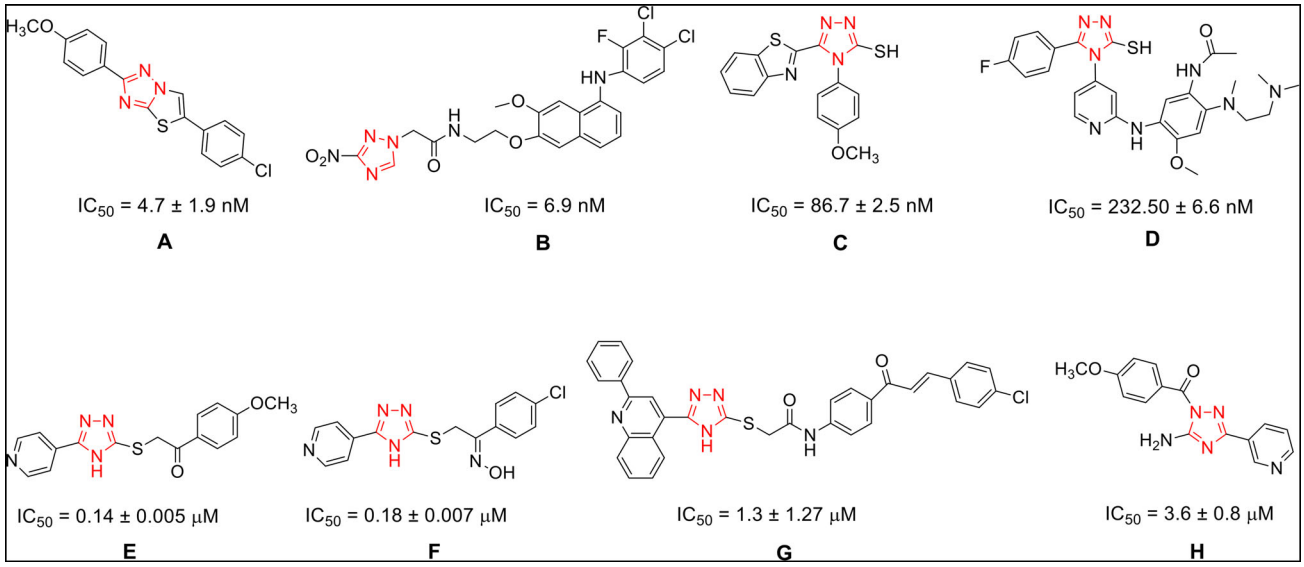

Figure 2. Some 1,2,4-triazole derivatives previously reported as EGFR inhibitors.

and vorozole are non-steroidal aromatase inhibitors used in the clinical treatment of breast cancer (Figure 1; Brueggemeier et al., 2005).

Thiosemicarbazides (TSC) are reactive intermediates with the functional group -NH-NH-CS-NH-, also called hydrazinecarbothioamides, which are generally formed by the reaction of hydrazides with isothiocyanates (Gultekin et al., 2021). These compounds show different pharmacological activities like antibacterial, antifungal, antituberculosis, antioxidant, antimalarial, antiviral, anticonvulsant and antiproliferative, as well as being also used as key products in the synthesis of heterocyclic compounds such as mercapto-1,2,4-triazole (Gultekin et al., 2021), 1,3,4-thiadiazole (Plech et al., 2014) and 1,3,4-oxadiazole (Ali et al., 2019).

Mercapto-1,2,4-triazoles, which are the basic cyclization products of TSC's constitute an important class among other heterocycles due to their use in pharmacological, industrial and medical studies (Küçükgüzel & Çıkla-Süzgün, 2015). These compounds and their metal complex have been reported to possess a wide variety of pharmacological and biological activities including antifungal, antibacterial, antimycobacterial, antiviral, anti-Parkinson's, anti-inflammatory, anticonvulsant, antidiabetic, anticancer and anti-parasitic agentes (Küçükgüzel et al., 2008; Küçükgüzel & Çıkla-Süzgün, 2015; Plech et al., 2014; Shaker, 2006). Apart from these, although it is known that 1,2,4-triazole derivatives exhibit good inhibitory potential against many enzymes such as monoamine oxidase (Bekircan et al., 2022), tyrosinase (Akin et al., 2019; Gultekin et al., 2021), carbonic anhydrase (Akin et al., 2019; Vats et al., 2019), urease (Akhtar et al., 2010) metallo-β-lactamase (Legru et al. 2021), lipase (Bekircan et al., 2015; Kumar & Chauhan, 2021), α-glucosidase and α-amylase (Bekircan et al., 2015; Channar et al., 2017) and there are limited studies on EGFR inhibitory activities (Figure 2; A: El-Sherief et al., 2018; B: Wei et al., 2019; C: Mokhtar et al. 2020; D: Yang et al., 2020; E and F: El-Wahab et al. 2021; G: Mohassab et al., 2021; H: El-Sherief et al., 2018)

In the light of this information, it has been determined that heterocycles containing nitrogen and sulphur have important pharmacological and enzyme inhibition properties. Therefore, the synthesis of new heterocyclic molecules carrying 3-aryl-5-alkyl-1*H*-1,2,4-triazole ring was aimed. Therefore, heterocyclic molecules carrying 5-[(1*H*-1,2,4-triazol-1-yl)methyl]-3*H*-1,2,4-triazole-3-thione structure were designed and screened *in silico* against hEGFR. Chemical structures of screened compounds are summarized in Figure 3 and elaborately defined in *Results and Discussion* part. After *in silico* evaluation, some of the selected compounds were synthesized and tested for hEGFR enzyme *in vitro*. At the end of the study, we've reached EGFR inhibitors with 5-[(1*H*-1,2,4-triazol-1-yl)methyl]-3*H*-1,2,4-triazole-3-thione structure at nanomolar range.

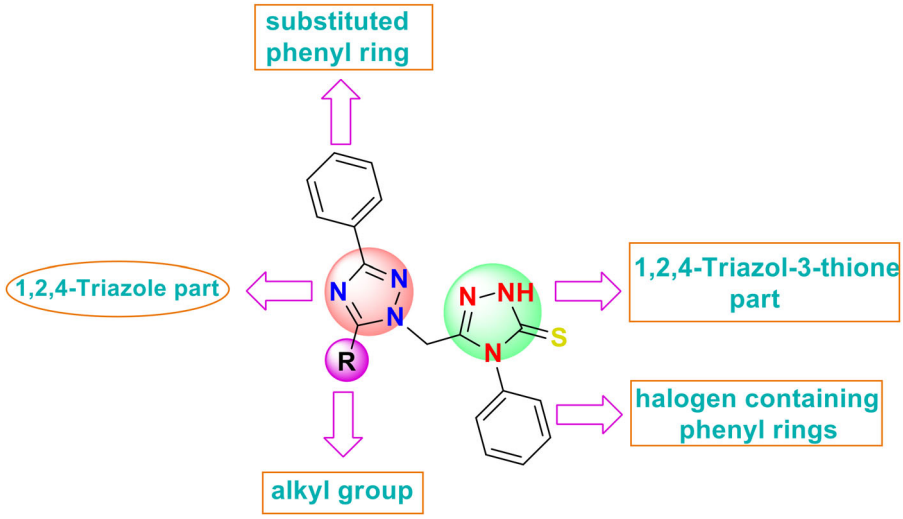

Figure 3. General structure of the compounds planned to be synthesized.

Materials and methods

Molecular modeling studies

Instruments

Molecular modeling studies were carried out on DELL Precision Power 6320 Workstation (Intel Xeaon CPU E3-1245 v6, 3.70 GHz x8). FlexX (LeadIT v2.3.2, BioSolveIT GmbH, St. Augustin, Germany) and MOE (v2016.0802, Chemical Computing Group Inc., Montreal) software were used to perform modeling studies.

Preparation of proteins

Crystal structures of hEGFR in complex with tak-285 (3POZ), lapatinib (1XKK) and gefitinib (4KWQ) were obtained from the RCSB Protein Data Bank. Water molecules, ions and buffer molecules were deleted from the structures. The remaining structures were protonated according to the protonate 3D protocol of the MOE package. Energy minimization was performed using AMBER14:EHT force field.

Preparation of ligands

3D structures of ligands in low-energy conformations were prepared using MOE. The most prevalent protonation state of the ligands at pH 7 was calculated. Energy minimization was conducted for all ligands using the steepest-descent protocol MMFF94x force field.

Molecular docking

Docking studies were performed using FlexX. Binding sites were defined as all residues within 6.5 Å of the cocrystallized ligands. All ligands were docked fifty times and the best-scoring three poses were subjected to refinement calculations. Energy minimization was conducted for docked ligands and amino acid residues in binding the pocket of protein using GBVI/WSA force field (Labute, 2008).

Chemistry

All chemicals used in the synthesis were purchased from Sigma-Aldrich, Merck, Acros Organics and ISOLAB companies. Melting points were determined with a Thermo Scientific digital 9200 series melting point apparatus. IR spectra were recorded on the Perkin-Elmer Frontier FTIR spectrophotometer using the ATR technique. The ^{1}H- and ^{13}C-NMR spectra were taken on a BrukerAVANCE III 400 MHz NMR spectrometer (400.13 MHz for 1H- and 100.13 MHz for 13C-) in dimethyl sulfoxide-d_6 solvent. The mass spectra were recorded on Agilent 1260 Infinity series Accurate-Mass Time-of-Flight (Q-TOF) LC/MS spectrometer.

Synthesis

General procedure for the synthesis of 3-aryl-5-alkyl-1H-1,2,4-triazoles (4a–c)

1.15 g (50 mmol) sodium were dissolved in 80 mL ethanol. 50 mmol of ethyl alkylimidate hydrochlorides (**1**) in 150 mL of ethanol were added at room temperature and the sodium chloride which precipitates out is filtered off. 40 mmol of suitable benzoic acid hydrazides (**2**) were added to the filtrate and the mixture was stirred overnight. The reaction mixture is concentrated and cooled. The precipitated solid (**3a–c**) was filtered off and washed with cold ethanol and dried and used for the next step without purification (Konetzki et al., 2006; Yılmaz & Mentese, 2014). Compounds **3a–c** were heated in an oil bath at 180 °C for 30 min under a solvent-free. After cooling, the solid was recrystallized from chloroform (Scheme 1; Konetzki et al., 2006; Yılmaz & Mentese, 2014).

3-Phenyl-5-methyl-1H-1,2,4,-triazole (4a). Yield: 72%; mp: 162–163 °C (Lit. (Francis et al., 1987) mp: 168–169 °C; Scheme 1).

5-Cyclopropyl-3-phenyl-1H-1,2,4-triazole (4b). Yield: 80%; mp: 196–198 °C (Lit. (Inturi et al., 2016) mp: 199.9–201.7 °C; Scheme 1).

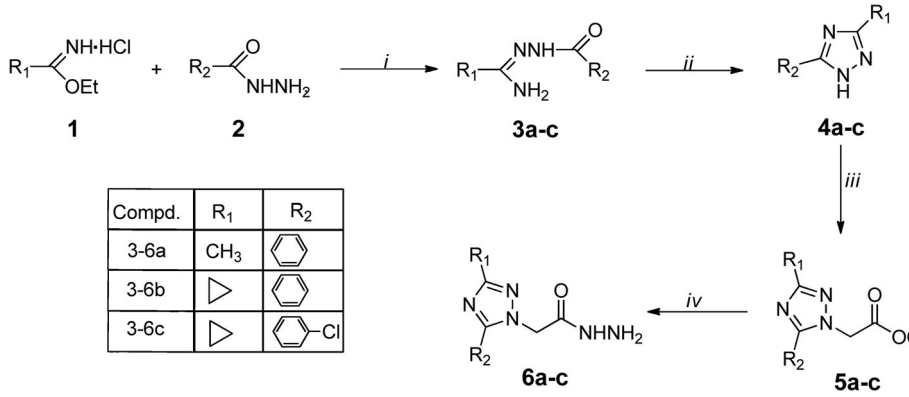

Scheme 1. Reagents and conditions: *i.* absolute ethanol, NaOEt; *ii.* Heated to 180 °C; *iii.* absolute ethanol, NaOEt/ethyl bromoacetate, reflux; *iv*. absolute ethanol, $NH_2NH_2{\cdot}H_2O$, reflux;

3-(4-Chlorophenyl)-5-cyclopropyl-1H-1,2,4-triazole (4c). Yield: 51%; mp: 204–205 °C (Lit. (Xia et al., 2019) mp: 202–203 °C; Scheme 1).

General procedure for the synthesis of ethyl acetate derivatives (5a–c)

To a solution of 3,5-disubstitute-1*H*-1,2,4-triazoles (**4a–c**) (10 mmol) in 50 mL of absolute alcohol was added metallic sodium solution (10 mmol) in 50 mL of absolute alcohol and refluxed for 2 h protected from moisture. After 2 h, ethyl bromoacetate (10 mmol) was added to the cooled mixture and the reaction was refluxed under the same conditions for another 12 h. The progression of the reaction was monitored by TLC. After this time, the cooled mixture was evaporated under reduced pressure, the remaining solid part was crystallized from aqueous ethanol (50%).

Ethyl-3-(phenyl)-5-methyl-1H-1,2,4-triazol-1-yl acetate (5a). Yield: 81%; mp: 85–86 °C. FT-IR (ν_{max}, cm^{-1}): 1748 cm^{-1} (C = O), 1528 cm^{-1} (C = N); ^{1}H-NMR (DMSO-d_6, δ ppm): 1.24 (t, 3H, *J* = 8.0 Hz CH_3), 2.43 (s, 3H, CH_3), 4.2 (q, 2H, *J* = 8.0 Hz, OCH_2), 5.22 (s, 2H, N-CH_2), Ar-H: [7.41–7.48 (m,3H), 7.97–7.98 (m, 2H)]; ^{13}C-NMR, APT (DMSO-d_6, δ ppm): 11.84 ($OCH_2\underline{CH_3}$), 14.45 (CH_3), 49.89 (N-CH_2), 61.97 (OCH_2), Ar-C: [126.06 (2CH), 129.18 (2CH), 129.51 (CH), 131.33], 155.02 (triazole C-5), 160.01 (triazole C-3), 167.97 (C = O).

Ethyl-3-(phenyl)-5-methyl-1H-1,2,4-triazol-1-yl acetate (5b). Yield: 57%; mp: 82–83 °C. FT-IR (ν_{max}, cm^{-1}): 1744 cm^{-1}(C = O), 1513 cm^{-1}(C = N); ^{1}H-NMR (DMSO-d_6, δ ppm): 0.97–1.09 (m, 4H, cyclopropyl $2CH_2$), 1.24 (t, 3H, *J* = 8.0 Hz CH_3), 2.12–2.19 (m, 1H, cyclopropyl CH), 4.2 (q, 2H, *J* = 8.0 Hz, OCH_2), 5.30 (s, 2H, N-CH_2), Ar-H: [7.39–7.45 (m, 3H), 7.91–7.93 (m, 2H)]. ^{13}C-NMR, APT (DMSO-d_6, δ ppm): 6.24 (cyclopropyl CH), 8.84 (cyclopropyl CH_2), 14.48(CH_3), 49.80 (N-CH_2), 61.90 (OCH_2), Ar-C: [126.11 (2CH), 129.11(2CH), 129.48(CH), 131.30], 159.83 (triazole C-5), 159.99 (triazole C-3), 168.00 (C = O).

Ethyl 3-(4-Chlorophenyl)-5-cyclopropyl-1H-1,2,4-triazol-1-yl acetate (5c). Yield: 54%; mp: 89–90 °C. FTIR (ν_{max}, cm^{-1}): 1735 (C = O), 1631 (C = N); ^{1}H-NMR (DMSO-d_6, δ ppm): 0.98–1.07 (m, 2H, cyclopropyl $2CH_2$), 1.23 (t, 3H, *J* = 8.0 Hz, CH_3), 2.15–2.18 (m, 1H, cyclopropyl CH), 4.2 (q, 2H, *J* = 8.0 Hz OCH_2), 5.31 (s, 2H, N-CH_2), Ar-H:: [7.50 (d, 2H, *J* = 8.0 Hz), 7.92 (d, 2H, *J* = 8.0 Hz)]; ^{13}C-NMR, APT (DMSO-d_6, δ ppm): 6.23 (cyclopropyl CH), 8.95 (cyclopropyl $2CH_2$), 14.47 (CH_3), 49.64 (N-CH_2), 61.94 (OCH_2), Ar-C: [127.84 (2CH), 129.25 (2CH), 130.13, 134.05), 158.90 (triazole C-5), 160.28 (triazole C-3), 167.94 (C = O).

General procedure for the synthesis of acetohydrazide derivatives (6a–c)

To a solution of ester derivatives (**4a–c**) (10 mmol) in 50 mL of 1-butanol was added hydrazine hydrate (1.24 mL, 25 mmol) and refluxed for 6 h. The progression of the reaction was monitored by TLC. At the end of this period, the cooled mixture was kept in the refrigerator (4 °C) for 12 h and the precipitated white solid was filtered, washed with petroleum ether, dried and crystallized from ethanol.

2-(5-Methyl-3-phenyl-1H-1,2,4-triazol-1-yl)acetohydrazide (6a). Yield: 79%; mp: 189–190 °C. FTIR (ν_{max}, cm^{-1}): 3290–3191 (NH + NH_2), 1659 (C = O), 1615 (C = N); ^{1}H-NMR (DMSO-d_6, δ ppm): 2.36–2.44 (s, 3H, CH_3), 4.39 (NH_2), 4.83 (N-CH_2), Ar-H: [7.39–7.46 (m, 3H), 7.93–7.96 (m, 2H)], 9.49 (s, 1H, NH); ^{13}C-NMR, APT (DMSO-d_6, δ ppm): 12.10 (CH_3), 49.82 (N-$\underline{CH_2}$), Ar-C: [125.99 (2CH), 129.14 (2CH), 129.37 (CH), 131.49], 155.05 (triazole C-5), 159.73 (triazole C-3), 165.79 (C = O);

2-(5-Cyclopropyl-3-phenyl-1H-1,2,4-triazol-1-yl)acetohydrazide (6b). Yield: 89%; mp: 155–156 °C. FTIR (ν_{max}, cm^{-1}): 3302–3247 (NH + NH_2), 1664 (C = O), 1612 (C = N); ^{1}H-NMR (DMSO-d_6, δ ppm): 0.98–1.06 (m, 4H, cyclopropyl $2CH_2$), 2.12–2.16 (m, 1H, cyclopropyl CH), 4.38 (s, 2H, NH_2), 4.92 (s, 2H, N-CH_2), Ar-H: [7.38–7.44 (m, 3H), 7.90 (d, 2H, *J* = 8.0 Hz)], 9.47 (s, 1H, NH); ^{13}C-NMR, APT (DMSO-d_6, δ ppm): 6.47 (cyclopropyl CH), 8.78 (cyclopropyl CH_2), 49.50 (N-CH_2), Ar-C: [126,05 (2CH), 129.06 (2CH), 129.33 (CH), 131.50], 159.58 (triazole C-5), 159.90 (triazole C-3), 165.76 (C = O);

2-[3-(4-Chlorophenyl)-5-cyclopropyl-1H-1,2,4-triazol-1-yl]acetohydrazide (6c). Yield: 71%; mp: 208–209 °C. FTIR (ν_{max}, cm^{-1}): 3163–3282 (NH + NH_2), 1655 (C = O), 1617 (C = N);

^{1}H-NMR (DMSO-d_6, δ ppm): 0.99–1.07 (m, 4H, cyclopropyl 2CH_2), 2.13–2.17 (m, 1H, cyclopropyl CH), 4.39 (s, 2H, NH_2), 4.93 (s, 2H, N-CH_2), Ar-H: [7.49 (d, 2H, $J = 8.0$ Hz), 7.91 (d, 2H, $J = 8.0$ Hz)], 9.49 (s, 1H, NH); ^{13}C-NMR, APT (DMSO-d_6, δ ppm): 6.46 (cyclopropyl CH), 8.99 (cyclopropyl cyclopropyl 2CH_2), 49.55 (N-CH_2), Ar-C: [127.78 (2CH), 129.21 (2CH), 130.33, 133,89], 158,66 (triazole C-5), 160.20 (triazole C-3), 165.71 (C = O).

General procedure for the synthesis of thiosemicarbazide derivatives (7a–h)

To a solution of acetohydrazide derivatives (**6a–c**) (10 mmol) in 50 mL of absolute ethanol was added suitable isothiocyanates (10 mmol) and refluxed for 6 h. The progression of the reaction was monitored by TLC. At the end of these periods, the mixture was left in the refrigerator (4 °C) for 12 h and the precipitated white solids were filtered, washed with petroleum ether, dried and crystallized from acetonitrile.

2-[(5-Methyl-3-phenyl-1H-1,2,4-triazol-1-yl)acetyl]-4-phenyl thiosemicarbazide (7a). Yield: 92%; mp: 179–180 °C. FTIR (ν_{max}, cm^{-1}): 3262 (NH), 1688 (C = O), 1598 (C = N); ^{1}H-NMR (DMSO-d_6, δ ppm): 2.45 (s, 3H, CH_3), 5.05 (s, 2H, N-CH_2), Ar-H: [7.18–7.22 (m, 1H), 7.34–7.47 (m, 7H), 7.96 (d, 2H, $J = 8.0$ Hz)], 9.75 (s, 2H, NH), 10.48 (s, 1H, NH); ^{13}C-NMR, APT (DMSO-d_6, δ ppm): 12.15 (CH_3), 49.96 (N-CH_2), Ar-C: [126.02 (4CH), 128.68 (CH), 129.16 (4CH), 129.42 (CH), 131.46, 139.41]. 155.22 (triazole C-5), 159.81 (triazole C-3), 166.46 (C = O), (C = S not observed); LC-QTOF-MS calculated for $C_{18}H_{18}N_6OS$ $[M + H]^+$: 367.1341, found 367.1379.

2-[(5-Methyl-3-phenyl-1H-1,2,4-triazol-1-yl)acetyl]-4-(3-methylphenyl)thiosemicarbazide (7b). Yield: 89%; mp: 151–152 °C. FTIR (ν_{max}, cm^{-1}): 3168 (NH), 1686 (C = O), 1608 (C = N); ^{1}H-NMR (DMSO-d_6, δ ppm): 2.30 (s, 3H, CH_3), 2.45 (s, 3H, CH_3), 5.04 (s, 2H, N-CH_2), Ar-H: [7.03–7.47 (m, 7H), 7.96 (d, 2H, $J = 8.0$ Hz)], 9,73 (s, 2H, NH), 10.48 (s, 1H, NH); ^{13}C-NMR, APT (DMSO-d_6, δ ppm): 12.16 (triazole CH_3), 21.41 (CH_3), 49.95 (N-CH_2), Ar-C: [126.02 (3CH), 126.59 (CH), 128.51 (CH), 129.18 (3CH), 129.35 (CH), 131.45, 137.93, 139.29], 155.23 (triazole C-5), 159.80 (triazole C-3), 166.49 (C = O), 181.33 (C = S); LC-QTOF-MS calculated for $C_{19}H_{20}N_6OS$ $[M + H]^+$: 381.1498, found 381.1541.

2-[(5-Methyl-3-phenyl-1H-1,2,4-triazol-1-yl)acetyl]-4-(4-chlorophenyl)thiosemicarbazide (7c). Yield: 80%; mp: 176–177 °C. FTIR (ν_{max}, cm^{-1}): 3158 (NH), 1692 (C = O), 1596 (C = N); ^{1}H-NMR (DMSO-d_6, δ ppm): 2.45 (s, 3H, CH_3), 5.04 (s, 2H, N-CH_2), Ar- H: [7.40–7.47 (m, 7H), 7.96 (d, 2H, $J = 8.0$ Hz)], 9.86 (s, 2H, NH), 10.50 (s, 1H, NH); ^{13}C-NMR, APT (DMSO-d_6, δ ppm): 12.15 (CH_3), 49.97 (N-CH_2), Ar-C: [126.02 (4CH), 128.60 (2CH), 129.16 (2CH), 129.42 (CH), 131.45, 138.36, 138.42], 155.22 (triazole C-5), 159.65 (triazole C-3), 167.71 (C = O), (C = S, not observed); LC-QTOF-MS calculated for $C_{18}H_{17}ClN_6OS$ $[M + H]^+$: 401.0951, found 401.0987.

2-[(5-Methyl-3-phenyl-1H-1,2,4-triazol-1-yl)acetyl]-4-(3-chlorophenyl)thiosemicarbazide (7d). Yield: 91%; mp: 158–159 °C. FTIR (ν_{max}, cm^{-1}): 3168 (NH), 1689 (C = O), 1591 (C = N); ^{1}H-NMR (DMSO-d_6, δ ppm): 2.45 (s, 3H, CH_3), 5.05 (s, 2H, N-CH_2), Ar-H: [7.41–7.45 (m, 7H), 7.96 (d, 2H, $J = 8.0$ Hz)], 9.94 (s, 2H, NH), 10.53 (s, 1H, NH); ^{13}C-NMR, APT (DMSO-d_6, δ ppm): 12.16 (CH_3), 49.95 (N-CH_2), Ar-C: [126.01 (3CH), 127.87, 129.18 (3CH), 129.45 (2CH), 130.30 (CH), 131.43, 140.95], 155.23 (triazole C-5), 159.80 (triazole C-3), 166.67 (C = O), 187.44 (C = S); LC-QTOF-MS calculated for $C_{18}H_{17}ClN_6OS$ $[M + H]^+$: 401.0951, found 401.0988.

2-[(5-Methyl-3-phenyl-1H-1,2,4-triazol-1-yl)acetyl]-4-(3-bromophenyl)thiosemicarbazide (7e). Yield: 88%; mp: 159–160 °C. FTIR (ν_{max}, cm^{-1}): FTIR (ν_{max}, cm^{-1}): 3156 (NH), 1689 (C = O), 1588 (C = N); ^{1}H-NMR (DMSO-d_6, δ ppm): 2.45 (s, 3H, CH_3), 5.05 (s, 2H, N-CH_2), Ar-H: [7.40–7.46 (m, 7H), 7.96 (d, 2H, $J = 8.0$ Hz)], 9.94 (s, 2H, NH), 10.53 (s, 1H, NH); ^{13}C-NMR, APT (DMSO-d_6, δ ppm): 12.15 (CH_3), 49.95 (N-CH_2), Ar-C: [121.00, 126.02 (3CH), 129.48 (3CH), 129.45 (2CH), 130.43 (CH), 131.43, 141.07], 155.23 (triazole C-5), 159.80 (triazole C-3), 167.05 (C = O), 186.06 (C = S); LC-QTOF-MS calculated for $C_{18}H_{17}BrN_6OS$ $[M + H]^+$: 445.0446 [M (^{79}Br)+ H]$^+$ and 447.0426 [M (^{81}Br)+ H]$^+$, found 445.0441 and 447.0470, respectively.

2-[(5-Cyclopropyl-3-phenyl-1H-1,2,4-triazol-1-yl)acetyl]-4-(4-chlorophenyl)thiosemicarbazide (7f). Yield: 84%; mp: 99–100 °C. FTIR (ν_{max}, cm^{-1}): 3219 (NH), 1684 (C = O), 1595 (C = N); ^{1}H-NMR (DMSO-d_6, δ ppm): 1.01–1.09 (m, 4H, cyclopropyl 2CH_2), 2.10 (bs, 1H, cyclopropyl CH), 5.14 (s, 2H, N-CH_2), Ar-H: [7.39–7.48 (m, 7H), 7.92 (d, 2H, $J = 8.0$ Hz)], 9.89 (s, 2H, NH), 10.52 (s, 1H, NH); ^{13}C-NMR, APT (DMSO-d_6, δ ppm): 6.55 (cyclopropyl CH), 8.82 (cyclopropyl CH_2), 49.62 (N-CH_2), Ar-C: [126.08 (2CH), 128.59 (2CH), 129.10 (3CH), 129.41 (2CH), 131.42, 133.04, 138.44], 159.65 (triazole C-5), 160.04 (triazole C-3), 167.74 (C = O), 181,62 (C = S); LC-QTOF-MS calculated for $C_{20}H_{19}ClN_6OS$ $[M + H]^+$: 427.1108, found 427.1157.

2-{[3-(4-Chlorophenyl)-5-cyclopropyl-1H-1,2,4-triazol-1-yl)]acetyl}-4-(4-chlorophenyl)thiosemicarbazide (7g). Yield: 82%; mp: 182–183 °C. FTIR (ν_{max}, cm^{-1}): 3360 (NH), 1697 (C = O), 1595 (C = N); ^{1}H-NMR (DMSO-d_6, δ ppm): 0.98–1.07 (m, 4H, cyclopropyl 2CH_2), 2.08 (s, 1H, cyclopropyl CH), 5.12 (s, 2H, N-CH_2), Ar-H:[7.41–7.49 (m, 6H), 7.90 (d, 2H, $J = 8.0$ Hz)], 9.84 (s, 2H, NH), 10.53 (s, 1H, NH); ^{13}C-NMR, APT (DMSO-d_6, δ ppm): 6.48 (cyclopropyl CH), 8.86 (cyclopropyl CH_2), 49.58 (N-CH_2), Ar-C: [127.84 (2CH), 128.64 (2CH), 129.26 (4CH), 130.08, 134.08, 138.31, 141.33], 158,77 (triazole C-5), 160.43 (triazole C-3), 167.90 (C = O) (C = S, not observed); LC-QTOF-MS calculated for $C_{20}H_{18}Cl_2N_6OS$ $[M + H]^+$: 461.0718, found 461.0756.

2-{[3-(4-Chlorophenyl)-5-cyclopropyl-1H-1,2,4-triazol-1-yl]acetyl}-4-(4-trifluoromethylphenyl)thiosemicarbazide (7h). Yield: 77%; mp: 188–189 °C. FTIR (ν_{max}, cm^{-1}): 3205 (NH), 1686 (C = O), 1605 (C = N); ^{1}H-NMR (DMSO-d_6, δ ppm): 1.01–1.09 (m, 4H cyclopropyl 2CH), 2.11 (m, 1H, cyclopropyl

CH), 5.15 (s, 2H, N-CH_2), Ar-H: [7.59 (d, 2H, $J = 8.0$ Hz), 7.73 (bs, 4H), 7.92 (d, 2H, $J = 8.0$ Hz)], 10.04 (s, 2H, NH), 10.57 (s, 1H, NH); ^{13}C-NMR, APT (DMSO-d_6, δ ppm): 6.54 (cyclopropyl CH), 8.90 (cyclopropyl CH_2), 49.70(N-CH_2), 124.76 (dd, $\underline{C}F_3$, $J_{C\text{-}F}$ = 271.0 Hz) Ar-C: [(125.75 (2CH), 127.81 (4CH), 129.24 (2CH), 130.26, 133.99, 136.99 (d, C, $J = 103$Hz), 133.99, 137.34, 143.26], 158.74 (triazol C-5), 160.33 (triazol C-3), 167,01 (C = O), (C = S, not observed); LC-QTOF-MS calculated for $C_{21}H_{18}ClF_3N_6OS$ $[M + H]^+$: 495.0982, found 495.1038.

General procedure for the synthesis of 1,2,4-triazol-3-thione derivatives (8a–h)

Thiosemicarbazide derivatives (**7a–h**) (10 mmol) were refluxed in 100 mL 2N NaOH solution for about 6 h. The end of the reaction was monitored by TLC (hexane:ethyl acetate, 3:1). Then, the resulting solution was cooled to room temperature and acidified to pH 3–4 with 37% HCl. The precipitated white solids were filtered, washed with cold water, dried and crystallized from ethanol:water (4:1).

5-[(5-Methyl-3-phenyl-1H-1,2,4-triazol-1-yl)methyl]-4-phenyl-2,4-dihydro-1,2,4-triazol-3-thione (8a). Yield: 74%; mp: 290–291 °C. FTIR (ν_{max}, cm^{-1}): 3128 (NH), 1591, 1582 (C = N); ^{1}H-NMR (DMSO-d_6, δ ppm): 2.06 (s, 3H, CH_3), 5.36 (N-CH_2), Ar-H: [7.26–7.51 (m, 8H), 7.86 (d, 2H, $J = 8.0$ Hz)], 14.08 (s, 1H, SH); ^{13}C-NMR, APT (DMSO-d_6, δ ppm): 11.41 (CH_3), 43.59 (N-CH_2), Ar-C: [126.13 (2CH), 128.13 (2CH), 129.31 (2CH), 129.56 (CH), 129.87 (2CH), 130.26 (CH), 131.11, 133.37], 147.69 (triazole 3-thione C-5), 154.53 (triazole C-5), 160.29 (triazole C-3), 169.21 (triazole 3-thione C-3); LC-QTOF-MS calculated for $C_{18}H_{16}N_6S$ $[M + H]^+$: 349.1235, found 349.1298.

5-[(5-Methyl-3-phenyl-1H-1,2,4-*triazol*-1-yl)methyl]-4-(3-methylphenyl)-2,4-dihydro-1,2,4-triazole-3-thione (8b). Yield: 87%; mp: 254–255 °C. FTIR (ν_{max}, cm^{-1}): 3089 (NH), 1607, 1577 (C = N); ^{1}H-NMR (DMSO-d_6, δ ppm): 2.03 (s, 3H, CH_3), 2.21 (s, 3H, CH_3), 5.36 (s, 2H, N-CH_2), Ar-H: [6.89–7.44 (m, 7H), 7.88 (d, 2H, $J = 8.0$ Hz)], 14.06 (s, 1H, SH); ^{13}C-NMR, APT (DMSO-d_6, δ ppm): 11.36 (CH_3), 21.08 (CH_3), 43.59 (N-$\underline{C}H_2$), Ar-C: [125.36 (CH), 126.10 (2CH), 128.45 (CH), 129.14 (2CH), 129.61 (2CH), 130.80 (CH), 131.12, 133.23, 139.53], 147.73 (triazole 3-thione C-5), 154.58 (triazole C-5), 160.28 (triazole C-3), 169.18 (triazol 3-thione C-3); LC-QTOF-MS calculated for $C_{19}H_{18}N_6S$ $[M + H]^+$: 363.1392, found 393.1447.

5-[(5-Methyl-3-phenyl-1H-1,2,4-*triazol*-1-yl)methyl]-4-(4-chlorophenyl)-2,4-dihydro-1,2,4-triazole-3-thione (8c). Yield: 83%; mp: 157–158 °C. FTIR (ν_{max}, cm^{-1}): 3100 (NH), 1601, 1574 (C = N); ^{1}H-NMR (DMSO-d_6, δ ppm): 2.19 (s, 3H, CH_3), 5.41 (s, 2H, N-CH_2), Ar-H: [7.35–7.58 (m, 7H), 7.84 (d,2H, $J = 8.0$ Hz)], 14.11 (s, 1H, SH); ^{13}C-NMR, APT (DMSO-d_6, δ ppm): 11.60 (CH_3), 43.64 (N-$\underline{C}H_2$), Ar-C: [126.12 (2CH), 129.13 (2CH), 129.55 (CH), 129.91(2CH), 130.38 (2CH), 131.06, 132.30 136.00], 147.63 (triazole 3-thione C-5), 154.54 (triazole C-5), 160.19 (triazole C-3), 169.18 (triazole 3-thione C-3); LC-QTOF-MS calculated for $C_{18}H_{15}ClN_6S$ $[M + H]^+$: 383.0846, found 383.0894.

5-[(5-Methyl-3-phenyl-1H-1,2,4-triazol-1-yl)methyl]-4-(3-chlorophenyl)-2,4-dihydro-1,2,4-triazole −3-thione (8d). Yield: 90%; mp: 249–250 °C. FTIR (ν_{max}, cm^{-1}): 3125 (NH), 1598, 1583 (C = N); ^{1}H-NMR (DMSO-d_6, δ ppm): 2.18 (s, 3H, CH_3), 5.43 (s, 2H, N-CH_2), Ar-H: [7.28–7.58 (m, 7H), 7.75 (d, 2H, $J = 8.0$ Hz)], 14.14 (s, 1H, SH); ^{13}C-NMR, APT (DMSO-d_6, δ ppm): 11.58 (CH_3), 43.61(N-$\underline{C}H_2$), Ar-C: [126.13 (2CH), 127.37 (CH), 128.50 (CH), 129.10 (2CH), 129.57 (CH), 130.34 (CH), 131.06, 131.36 (CH),133.89, 134.63], 147.60 (triazole 3-thione C-5), 154.56 (triazole C-5), 160.28 (triazole C-3), 169.14 (triazole 3-thione C-3); LC-QTOF-MS calculated for $C_{18}H_{15}ClN_6S$ $[M + H]^+$: 383.0846, found 383.0912.

5-[(5-Methyl-3-phenyl-1H-1,2,4-triazol-1-yl)methyl]-4-(3-bromophenyl)-2,4-dihydro-1,2,4-triazole-3-thione (8e). Yield: 78%; mp: 273–274 °C. FTIR (ν_{max}, cm^{-1}): 3125 (NH), 1601, 1583 (C = N); ^{1}H-NMR (DMSO-d_6, δ ppm): 2.18 (s, 3H, CH_3), 5.43 (s, 2H, N-CH_2), Ar-H: [7.32–7.70 (m, 7H), 7.84 (s, 2H)], 14.14 (s, 1H, SH); ^{13}C-NMR, APT (DMSO-d_6, δ ppm): 11.59 (CH_3), 43.60 (N-$\underline{C}H_2$), Ar-C: [122.07, 126.16 (2CH), 127.73 (CH), 129.10 (2CH), 129.57 (CH), 131.06, 131.24 (CH), 131.58(CH), 133.21(CH), 134.72], 147.60 (triazole 3-thione C-5), 154.55 (triazole C-5), 160.30 (triazole C-3), 169.14 (triazole 3-thione C-3); LC-QTOF-MS calculated for $C_{18}H_{15}BrN_6S$: 427.0341 [M (^{79}Br)+ H]$^+$ and 429.0320 [M (^{81}Br)+ H]$^+$, found 427.0391 and 429.0374, respectively.

5-[(5-Cyclopropyl-3-phenyl-1H-1,2,4-triazol-1-yl)methyl]-4-(4-chlorophenyl)-2,4-dihydro-1,2,4-triazole −3-thione (8f). Yield: 79%; mp: 163–164 °C. FTIR (ν_{max}, cm^{-1}): 3150 (NH), 1601, 1582 (C = N); ^{1}H-NMR (DMSO-d_6, δ ppm): 0.79–0.97 (m, 4H, cyclopropyl 2 CH_2), 1.85–1.88 (m, 1H, cyclopropyl CH), 5.54 (N-CH_2), Ar-H: [7.28–7.55 (m, 7H), 7.79 (d, 2H, $J = 8.0$ Hz)], 14.12 (s, 1H, SH); ^{13}C-NMR, APT (DMSO-d_6, δ ppm): 6.09 (siklopropil CH), 9.20 (siklopropil CH_2), 43.41 (N-$\underline{C}H_2$), Ar-C: [126.19 (2CH), 129.07 (2CH), 129.54 (CH), 129.99 (2CH), 130.11 (2CH), 131.02, 132.20, 134.97], 147.80 (triazole 3-thione C-5), 159.57 (triazole C-5), 160.08 (triazole C-3), 169.17 (triazole 3-thione C-3); LC-QTOF-MS calculated for $C_{20}H_{17}ClN_6S$ $[M + H]^+$: 409.1002, found 409.1044.

5-{[3-(4-Chlorophenyl)-5-cyclopropyl-1H-1,2,4-triazol-1-yl] methyl}-4-(4-chlorophenyl)-2,4-dihydro-1,2,4-triazole-3-thione (8g). Yield: 81%; mp: 139–140 °C. FTIR (ν_{max}, cm^{-1}): 3100 (NH), 1609, 1578 (C = N); ^{1}H-NMR (DMSO-d_6, δ ppm): 0.79–0.97 (m, 4H, cyclopropyl 2CH_2), 1.86–1.89 (m, 1H, cyclopropyl CH), 5.56 (s, 2H, CH_2), Ar-H: [7.30 (d, 2H, $J = 8.0$ Hz), 7.47 (d, 2H, $J = 8.0$ Hz), 7.53 (d, 2H, $J = 8.0$ Hz), 7.80 (d, 2H, $J = 8.0$ Hz)] , 14.13 (s, 1H, SH); ^{13}C-NMR, APT (DMSO-d_6, δ ppm): 6.11 (cyclopropyl CH), 9.28 (cyclopropyl CH_2), 43.39 (N-$\underline{C}H_2$), Ar–C: [127.92 (2CH), 129.19 (2CH),129.86, (130.05 (d, 4CH, $J = 130$ Hz) 132.19, 134.14, 134.98], 147.71 (triazole 3-thione C-5), 159.14 (triazole C-5), 159.82 (triazole C-3), 169.20 (triazole 3-thione C-3); LC-QTOF-MS calculated for $C_{20}H_{16}Cl_2N_6S$ $[M + H]^+$: 443.0612, found 443.0668.

5-{[3-(4-Chlorophenyl)-5-cyclopropyl-1H-1,2,4-triazol-1-yl]

methyl}-4-(4-trifluoromethylphenyl)-2,4-dihydro-1,2,4-triazole-3-thione (8h). Yield: 76%; mp: 128–129 °C. FTIR (ν_{max}, cm^{-1}): 3126 (NH), 1615, 1578 (C = N); ^{1}H-NMR (DMSO-d_6, δ ppm): 0.74–0.95 (m, 4H, cyclopropyl 2 CH_2), 1.88 (s, 1H, cyclopropyl CH), 5.60 (s, 2H, N-CH_2), Ar- H: [7.49 (dd, 4H, J = 8.0 Hz), 7.80 (dd, 4H, J = 8.0 Hz), 14.21 (s, 1H, SH); ^{13}C-NMR, APT (DMSO-d_6, δ ppm): 6.05 (cyclopropyl CH), 9.26 (cyclopropyl 2CH_2), 43.42 (N-$\underline{C}H_2$), 124.20 (dd, $\underline{C}F_3$, $J_{C\text{-}F}$= 271,0 Hz) Ar-C: [127.03 (d, 2$\underline{C}$H, J = 4.0 Hz), 127.87 (2CH), 129.15 (2CH), 129.38 (2CH), 129.80, 130.38 (dd, $\underline{C}$, $J_{C\text{-}F}$= 32.0 Hz), 134.14, 136.91] , 147.59 (triazole 3-thione C-5), 159.13 (triazole C-5), 159.81 (triazole C-3), 169.12 (triazole 3-thione C-3); LC-QTOF-MS calculated for $C_{21}H_{16}ClF_3N_6S$ $[M+H]^+$: 477.0876, found 477.0935.

Enzyme activity and inhibition studies

Activity studies

Enzyme activity measurements were performed using TAKARA Universal Tyrosine Kinase Assay Kit and Wash and Stop Solution for ELISA Without Sulfuric Acid (Olgen et al., 2008) with some modifications. The enzyme (EGFR active human, sigma) used in the study was purchased commercially. Before starting the inhibition studies, the kit was characterized in terms of optimum enzyme and substrate concentration to be added to the medium. For this purpose, the enzyme activity reaction was carried out on a 96-well plate, the surface of which was previously coated. In order to determine the activity, 40 µL of enzyme was added to each well on the plate. Then, 10 µL of ATP-2Na solution was added to each well and incubated at 37 °C for 30 min. Addition of the ATP solution initiates the phosphorylation of Tyrosine. Afterwards, the solution was removed from the well and the wells were washed four times with the washing buffer included in the kit. Following this procedure, 100 µL of blocking solution was added and incubated at 37 °C for 30 min. The blocking solution was discarded and the wells were washed again with wash buffer. Again, 50 µL of anti-phosphotyrosine (PY20-HRP) solution was added to each well and incubated at 37 °C for 30 min. After this process, the antibody solution was removed and the wells were washed four times with the washing solution. 100 µL of HRP substrate solution (TMBZ) was also added to each well. The plate was incubated at 37 °C for approximately 15 min. 100 µL of stop solution was added to the wells in the same sequence in which the substrate solution was added. Activity was measured at 450 nm.

In the first stage, the optimum concentration of the enzyme to be used in the study was determined. Accordingly, activity measurements were made at constant substrate concentration and optimum pH and temperature values (determined by the manufacturer) with enzyme concentration in the range of 0.0007–0.1 µg/mL. The optimum enzyme concentration to be used in the kit was calculated from the data obtained as a result of these studies.

In the determination of the optimum substrate concentration and some kinetic parameters of the enzyme, enzyme activity was determined in the presence of ATP-2Na substrate with a final concentration ranging from 0.005 to 5 mM and in the reactions carried out under optimum enzyme, pH and temperature conditions. Since another substrate, poly (Glu-Tyr) (KVEKIGEGTYGVVYK: 6–20 residues of p34cdc2), was immobilized in the wells in the purchased commercial kit, the concentration of this substrate could not be changed. K_m and V_{max} values were calculated by plotting Lineweaver–Burk graph (Lineweaver & Burk, 1934) from the results obtained.

Inhibition studies

In the studies to determine the inhibition potentials of the synthesized molecules on hEGFR, the solutions of different concentrations were prepared by dissolving the molecules with DMSO. The volumes were adjusted so that the solvent amount in the reaction medium was 3% and pre-incubated with the enzyme (Copeland, 2005). A similar procedure was repeated only in the presence of this solvent to determine the effect of DMSO on the enzyme. With the results obtained, a graph of % Relative Activity versus inhibitor concentration was plotted for each synthesized molecule and the inhibitor concentration at which the activity decreased by 50% was determined as IC_{50} value. Lineweaver–Burk graphs were drawn from the results obtained, and K_m and V_{max} values were calculated in the presence and absence of inhibitor. The inhibition type was determined from these plots and the K_i value was calculated mathematically.

Results and discussion

Docking

Molecular modeling studies

In order to develop potential hEGFR inhibitors, molecular docking studies using crystal structures of the kinase domain (e.g., 3POZ, 1XKK and 4WKQ) were performed in the current study and several 5-[(1*H*-1,2,4-triazol-1-yl)methyl]-3*H*-1,2,4-triazole-3-thione derivatives were suggested for synthesis.

Design of virtual library containing 5-[(1H-1,2,4-triazol-1-yl)methyl]-3H-1,2,4-triazole-3-thione derivatives

For the computer-aided design of potential hEGFR kinase inhibitors, 297 5-[(1*H*-1,2,4-triazol-1-yl)methyl]-3*H*-1,2,4-triazole-3-thione derivatives in total were evaluated *in silico*. The 3rd and 5th positions of 1*H*-1,2,4-triazole ring and the 4th position of 3*H*-1,2,4-triazole-3-thione ring were derivatized. Methyl and cyclopropyl groups as alkyl group substituents and phenyl ring as aromatic substituent were examined at the 5th positions of 1*H*-1,2,4-triazole ring. Phenyl ring and 4-chloro and 4-methoxy substitutions of this phenyl ring were analyzed at the 3rd position of 1*H*-1,2,4-triazole heterocycle.

Diverse substitution at the 4th position of 3*H*-1,2,4-triazole-3-thione ring including alkyl and aryl groups was studied. Small or bulky groups from methyl substitution to 4-chlorophenethyl substitution were considered as alkyl groups. Activating groups like methyl or methoxy and

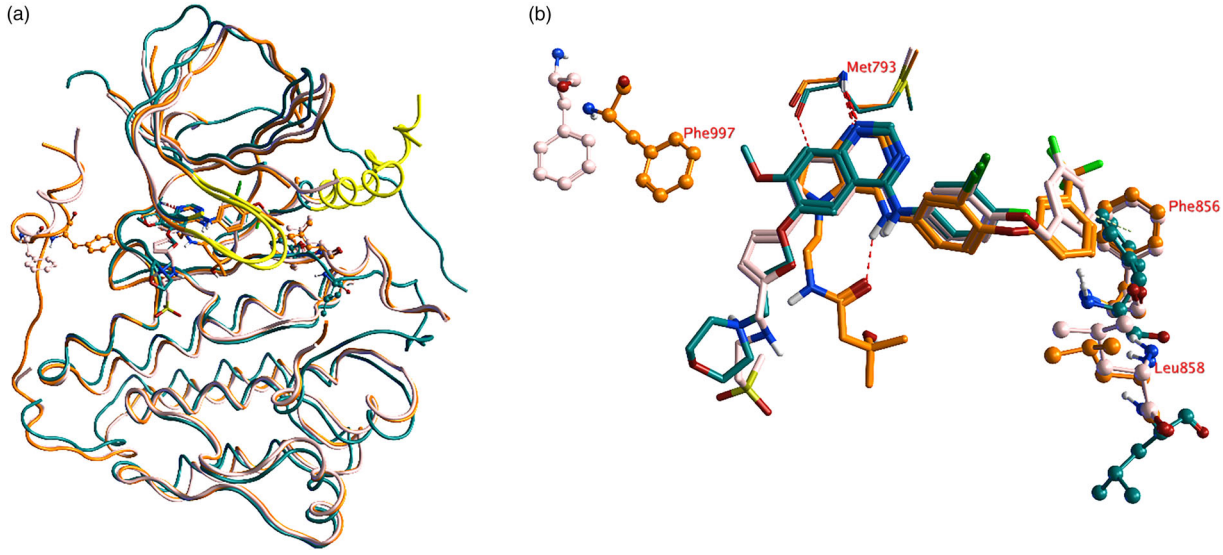

Figure 4. Comparison of the overall structure (a) and active site (b) of the hEGFR crystal structures. 3POZ co-crystallized with tak-285 is indicated in orange, 1XKK co-crystallized with lapatinib is indicated in green and 4WKQ co-crystallized with gefitinib is indicated in salmon. Loop between Val726-Ser720 and α-helical region between Lys754-Val765 are indicated in yellow.

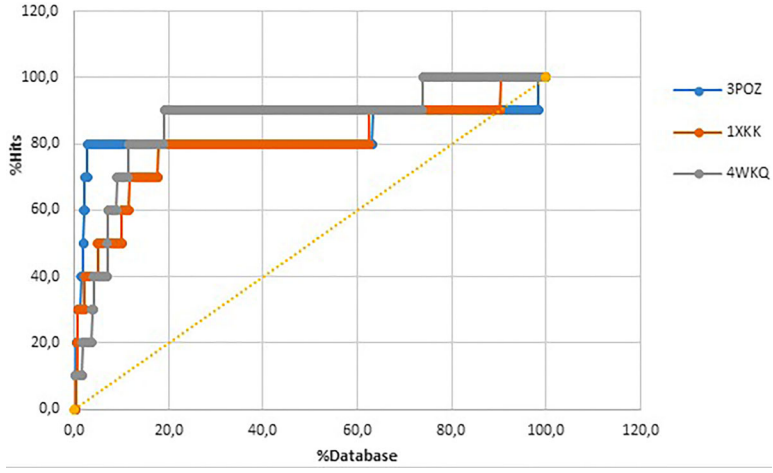

Figure 5. Enrichment graphs for 3POZ, 1XKK and 4WKQ.

deactivating groups like halogens, nitro, trifluoromethyl and trifluoromethoxy were investigated in the phenyl substitution of 4th position 3*H*-1,2,4-triazole-3-thione heterocycle. For the total list of scanned compounds, please refer to Supplementary Material Table S1.

Differences between the 3POZ, 1XKK and 4WKQ structures

Different co-crystal structures of hEFGR protein were extensively evaluated before docking calculations. 3POZ structure complexed with tak-285, 1XKK structure complexed with lapatinib and 4WKQ structure complexed with gefitinib were analyzed. Structural dissimilarities are shown in Figure 4. In detail, Phe997 is has a different orientation in the 3POZ and 1XKK crystal structures, while it is not resolved in the 4WKQ crystal structure (Figure 4). In 3POZ, this residue is close to the binding pocket, while in 1XKK it is located far away from the binding pocket due to conformational changes of the protein. The Phe856 amino acid is oriented differently in the 1XKK protein compared to the others. This difference is significant as this residue is located in the DFG (phenylalanine, glycine, aspartic acid) region of the activation loop of kinase proteins. In addition, there are significant differences in the loop between Val726-Ser720 region and Methyl, cyclopropyl or phenyl ring can be considered α-helical region between Lys754-Val765.

Validation of docking protocol

Retrospective docking studies of the three crystal structures were performed and the especially the key binding interactions between ligand and protein were correctly predicted (Supplementary Material Figures S1–S3).

Afterwards, 10 known actives together with 990 decoys (with similar properties as the actives; Supplementary Material Table S2) were docked into the binding pockets of all three crystal structures (Figure 5). For the 3POZ structure, 80% of the actives were found in the top 3.3% of the database. Similarly, 50% of the actives were found in the top 5.0% of the database for 1XKK and 60% of the actives were found in the top 7.7% of the database for 4WKQ.

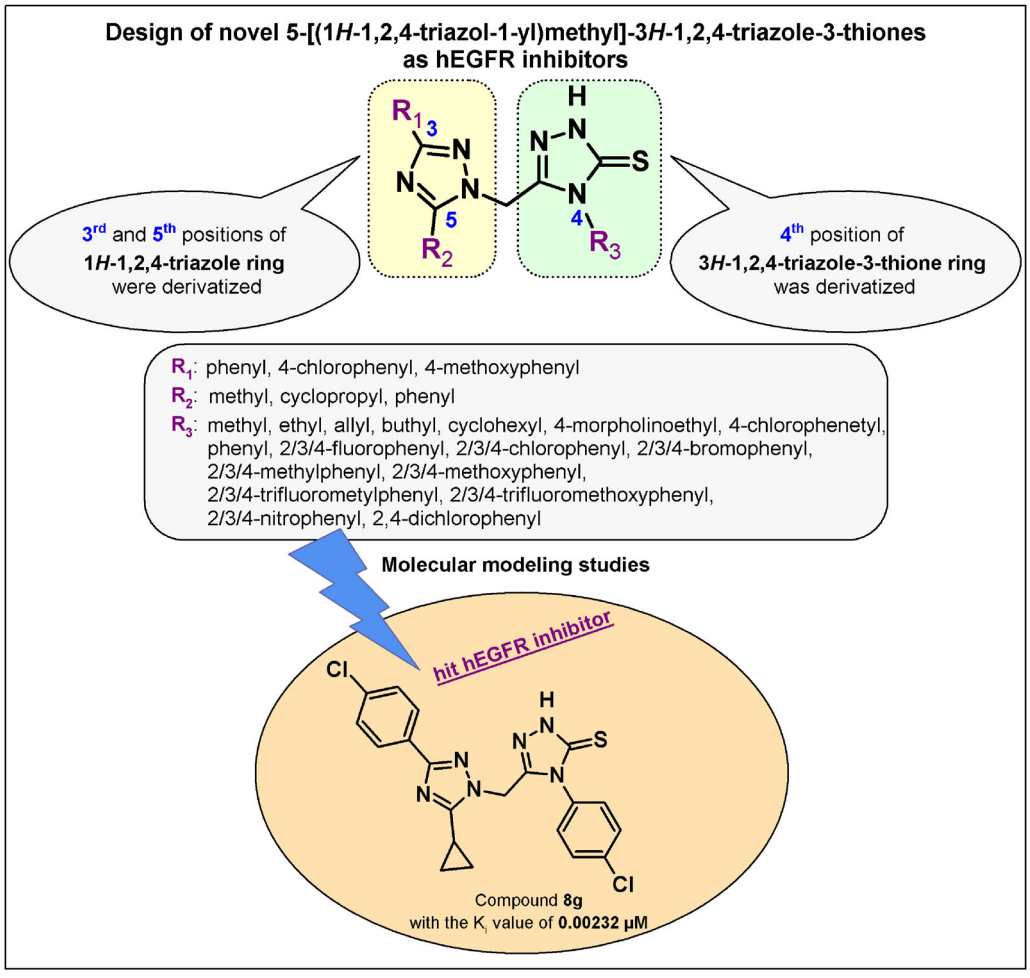

Figure 6. Summary of the design concept of novel 5-[(1*H*-1,2,4-triazol-1-yl)methyl]-3*H*-1,2,4-triazole-3-thione analogs as potent hEGFR inhibitors.

Docking of 5-[(1H-1,2,4-triazol-1-yl)methyl]-3H-1,2,4-triazole-3-thione derivatives against. Subsequently, the virtual database containing the 5-[(1*H*-1,2,4-triazol-1-yl)methyl]-3*H*-1,2,4-triazole-3-thione derivatives (Supplementary Material Table S1) was docked into all three crystal structures.

A total of 297 5-[(1*H*-1,2,4-triazol-1-yl)methyl]-3*H*-1,2,4-triazole-3-thione derivative compounds were scanned using the FlexX docking program. After the virtual screening, compounds were first searched for hydrogen bonding with the Met793 amino acid residue located in the hinge region of the hEGFR protein. 3D conformations of the molecules in the active sites of the proteins were examined.

Docking studies showed that C = S and N-H groups of 3*H*-1,2,4-triazole-3-thione ring may form hydrogen bond with Met793 amino acid residue. 3*H*-1,2,4-triazole-3-thione ring may act as hydrogen bond donor and acceptor both. Hydrophobic interaction may be observed between Gly796 residue and 3*H*-1,2,4-triazole-3-thione ring. As the 4th position of 3*H*-1,2,4-triazole-3-thione ring is suitable for the substitution of phenyl ring, the phenyl ring may occupy the hydrophobic allosteric site. This phenyl ring is also suitable for hydrophobic substitution, for instance, methyl, chloro, bromo or trifluoromethyl substituents. As for the 1*H*-1,2,4-triazole ring, the 3rd and 5th position of the 1*H*-1,2,4-triazole ring is suitable for substitution. Methyl and cyclopropyl ring can be considered at the 5th position.

Eventually, Figure 6 summarizes the design concept of novel 5-[(1*H*-1,2,4-triazol-1-yl)methyl]-3*H*-1,2,4-triazole-3-thione derivatives as potent hEGFR inhibitors. In light of modeling studies, it can be said that phenyl or substituted phenyl groups at R_1 position can promote hEGFR inhibitory activity. While methyl, cyclopropyl or phenyl groups can be tolerated at R_2 position, cyclopropyl or phenyl groups are preferred to increase hydrophobic interactions. Moreover, aromatic substitution is wanted at R_3 position to settle in hydrophobic pocket of hEGFR.

As a result of these comprehensive modeling studies, the synthesis of numerous heterocyclic compounds bearing 5-[(1*H*-1,2,4-triazol-1-yl)methyl]-3*H*-1,2,4-triazole-3-thione ring was suggested. As of suggested compounds, eight of them were synthesized and tested for hEGFR inhibitory activity. These compounds exhibited hEGFR inhibition at the nanomolar range. Representative conformation of the suggested compounds is presented in Figure 7.

Figure 7 shows 3D conformation of **8g** in the active site of 3POZ protein crystal from two different perspectives and Figure 8 demonstrates interactions between **8g** and 3POZ in 2D. As can be seen, **8g** settles very well in the active site of hEGFR. 3*H*-1,2,4-triazole-3-thione ring of **8g** forms two hydrogen bonds with Met793 amino acid residue at the hinge region. 1*H*-1,2,4-triazole ring of **8g** forms another hydrogen

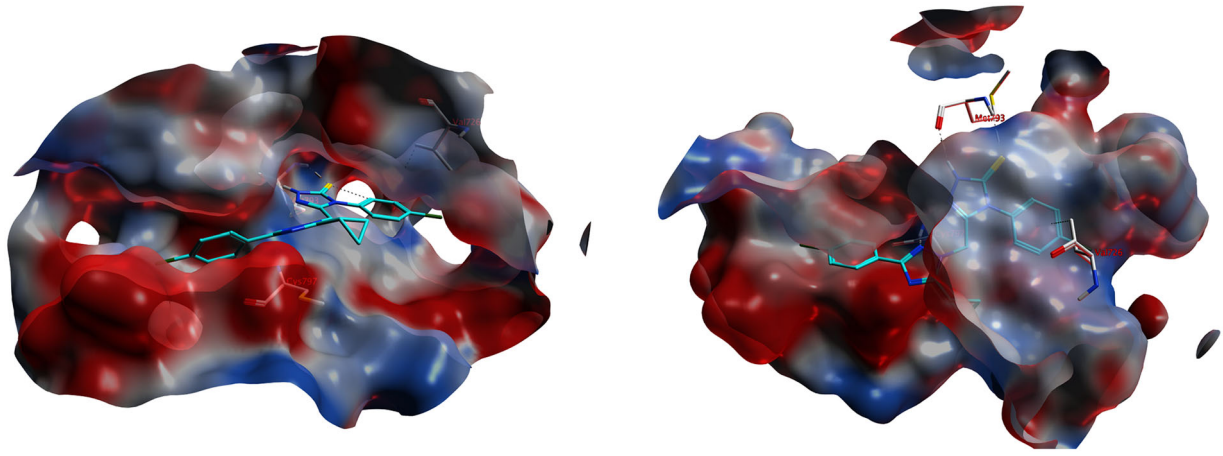

Figure 7. Representative presentation of suggested compounds in the active site of hEGFR (3POZ) from two different orientations. Compound **8g** is shown in cyan sticks.

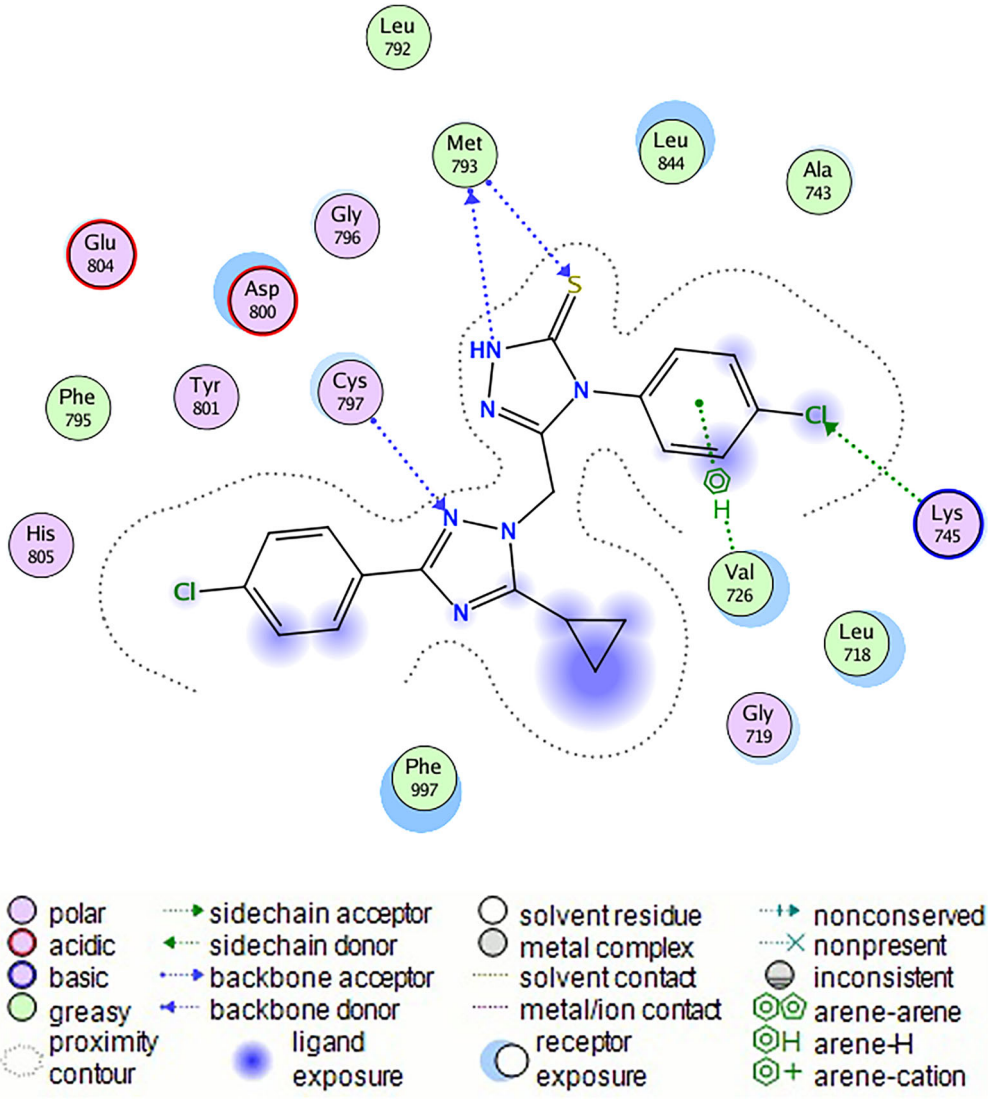

Figure 8. Molecular interactions between compound **8g** and 3POZ in 2D.

bond with Cys797. The phenyl ring at 4th position of 3*H*-1,2,4-triazole-3-thione ring shows arene-H interactions with Val726. Chlorine atom at the 4th position of the phenyl ring acts as sidechain acceptor of basic Lys745 amino acid residue.

It is remarkable to say that **8g**, which had the best score according to docking studies with 3POZ and 1XKK crystals showed the highest inhibitory activity against hEGFR activity. **8g** and the other two most active compounds **8c** and **8f** possess 4-chlorophenyl substituent at the 4th position of 3*H*-

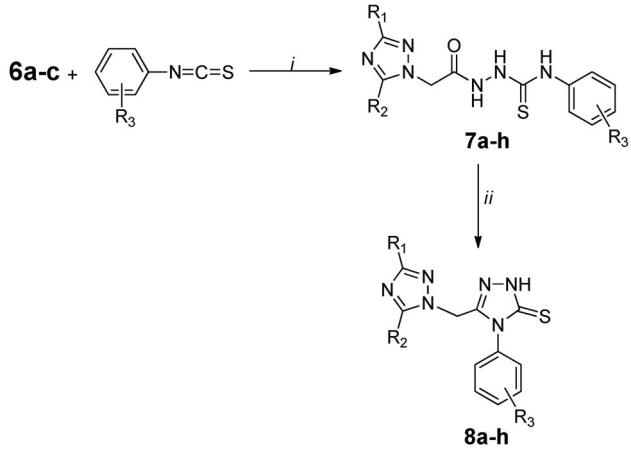

Compd.	R_1	R_2	R_3
7,8a	CH_3		H
7,8b	CH_3		3-CH_3
7,8c	CH_3		4-Cl
7,8d	CH_3		3-Cl
7,8e	CH_3		3-Br
7,8f			4-Cl
7,8g		Cl	4-Cl
7,8h		Cl	4-CF_3

Scheme 2. Reagents and conditions: *i.* absolute ethanol, reflux; *ii.* 2 N NaOH, reflux

1,2,4-triazole-3-thione ring. While **8c** has methyl substituent at 5th position of 1*H*-1,2,4-triazole ring, **8f** and **8g** have cyclopropyl at that position. As **8c** and **8f** have phenyl substituent at the 3rd position of 1*H*-1,2,4-triazole ring, **8g** has 4-chlorophenyl substituent at that position.

Chemistry

The intermediate and target compounds were synthesized according to the reactions outlined in Schemes 1 and 2. The structures of the synthesized compounds were elucidated using FTIR-ATR, ^{1}H-NMR, ^{13}C-NMR and mass spectral analysis techniques.

The first key intermediate, 1H-1,2,4-triazoles (**4a–c**), was prepared according to reported literatures and their structures were confirmed by matching their physical characteristics with those reported (Konetzki et al., 2006; Yılmaz & Mentese, 2014). The second key intermediate, acetohydrazide derivatives (**6a–c**), were synthesized from the treatment of ethylacetate derivatives (**5a–c**) with hydrazine hydrate in 1-butanol. In the IR spectrum ester C = O stretching bands around 1740 cm^{-1} disappeared, instead hydrazide C = O stretching bands were observed at about 1660 cm^{-1}. In the ^{1}H-NMR spectrum, the peaks at 1.16 ppm (quartet) and 4.08 ppm (triplet) belonging to the OCH_2CH_3 ster group disappeared, and the singlet peaks of NH_2 and NH protons of hydrazides were observed at about 4.39 and 9.49 ppm, respectively. Also, the hydrazide C = O peaks were seen at about 165 ppm in the ^{13}C-NMR spectrum. Thiosemicarbazides (**7a–h**) were obtained from the reaction of hydrazides (**6a–c**) with phenyl substituted isothiocyanates. The IR spectra of compounds **7a–h** have characteristic NH and C = O stretching bands of the thiosemicarbazide part at 3083–3202 cm^{-1}, 1667–1709 cm^{-1}, respectively. In the ^{1}H NMR spectra of **7a–h** derivatives, two NH protons in the range of 9.73–10.04 ppm and one NH protons in the range of 10.48–10.57 ppm were observed. In ^{13}C-NMR, thiosemicarbazide C = O and C = S carbon peaks were observed at about 166 ppm, and in the range of 181–187 ppm, respectively. Intramolecular cyclization of **7a–h** compounds in the presence of 2 N $NaOH_{(aq)}$ to give 5-[(3-aryl-5-alkyl-1H-1,2,4-triazol-1-yl]methyl}-4-(substitutedphenyl)-2,4-dihydro-1,2,4-triazole-3-thiones (**8a–h**). In the ^{1}H-NMR spectrum, the characteristic three NH singlet peaks of compounds **7a–h** between 9.73 and 10.57 ppm disappeared, instead singlet SH spectra at about 14 ppm were recorded. The C-5 and C-3 carbons of the 1,2,4-triazole-3-thiol ring appeared at about 147 and 169 ppm in the ^{13}C-NMR spectra. In addition, mass spectroscopic data also supports the accuracy of the proposed structures.

hEGFR activity studies

Determination and optimization of enzyme activity

ELISA kit was used as the activity method to examine the effect of synthesized molecules on hEGFR activity. It is stated in the literature that the ELISA method is used in the measurement of EGFR activity and inhibition, and the results obtained are comparable and reliable with radioactive method (Abou-Seri, 2010; Ma et al., 2016; Varkondi et al., 2005).

In order to determine the inhibition potentials of synthesized organic molecules on hEGFR, first of all, the optimum concentration of the enzyme in the reaction medium was determined. For this purpose, a series of activity assays in the concentration range of 0.0007–0.1 μg/mL were performed using the ELISA kit, and the optimum enzyme concentration was found to be 0.01 μg/mL from the results obtained. In previous studies in the literature with different kits, the amount of enzyme added to the reaction medium was reported as 50 ng/mL (Li et al., 2021), 15 μg/mL (Kang et al., 2013) and 100 ng/mL (Lü et al., 2013).

To determine the optimum substrate concentration in the reaction medium, enzyme activity was determined in the presence of ATP-2Na substrate varying in the concentration range of 0.005–5 mM and under other optimum conditions (optimal enzyme concentration, pH and temperature). K_m and V_{max} values were determined by drawing Lineweaver–Burk graph based on the results obtained. As a result of this study, the optimum substrate concentration at which the enzyme showed the best activity was found to be 0.5 mM. K_m and V_{max} values were calculated as 1.167 mM and 1666.6 μmol/min, respectively, from the Lineweaver–Burk plot. As a result of the literature search, no enzyme kinetic study was found for EGFR in the presence of ATP as a substrate. Other solutions were used at the concentration specified by the manufacturer.

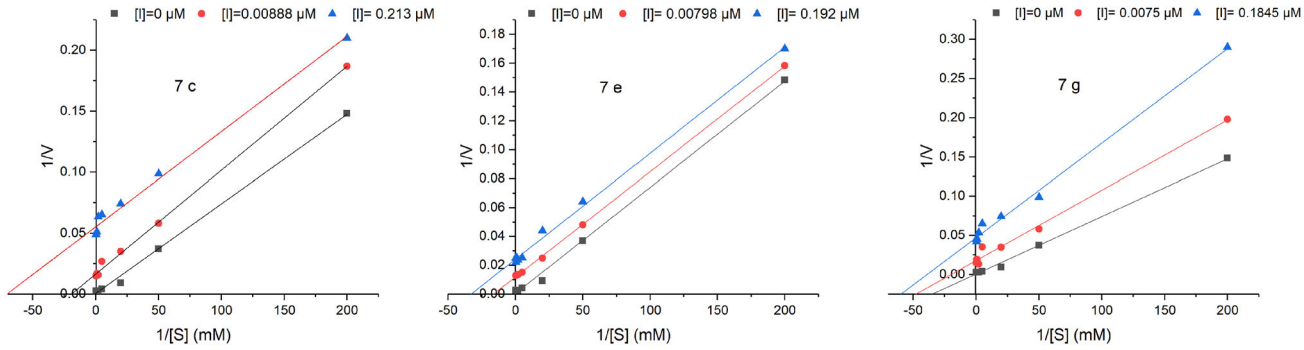

Figure 9. Lineweaver–Burk plots drawn to determine the inhibition types of **7c**, **7e** and **7g** molecules.

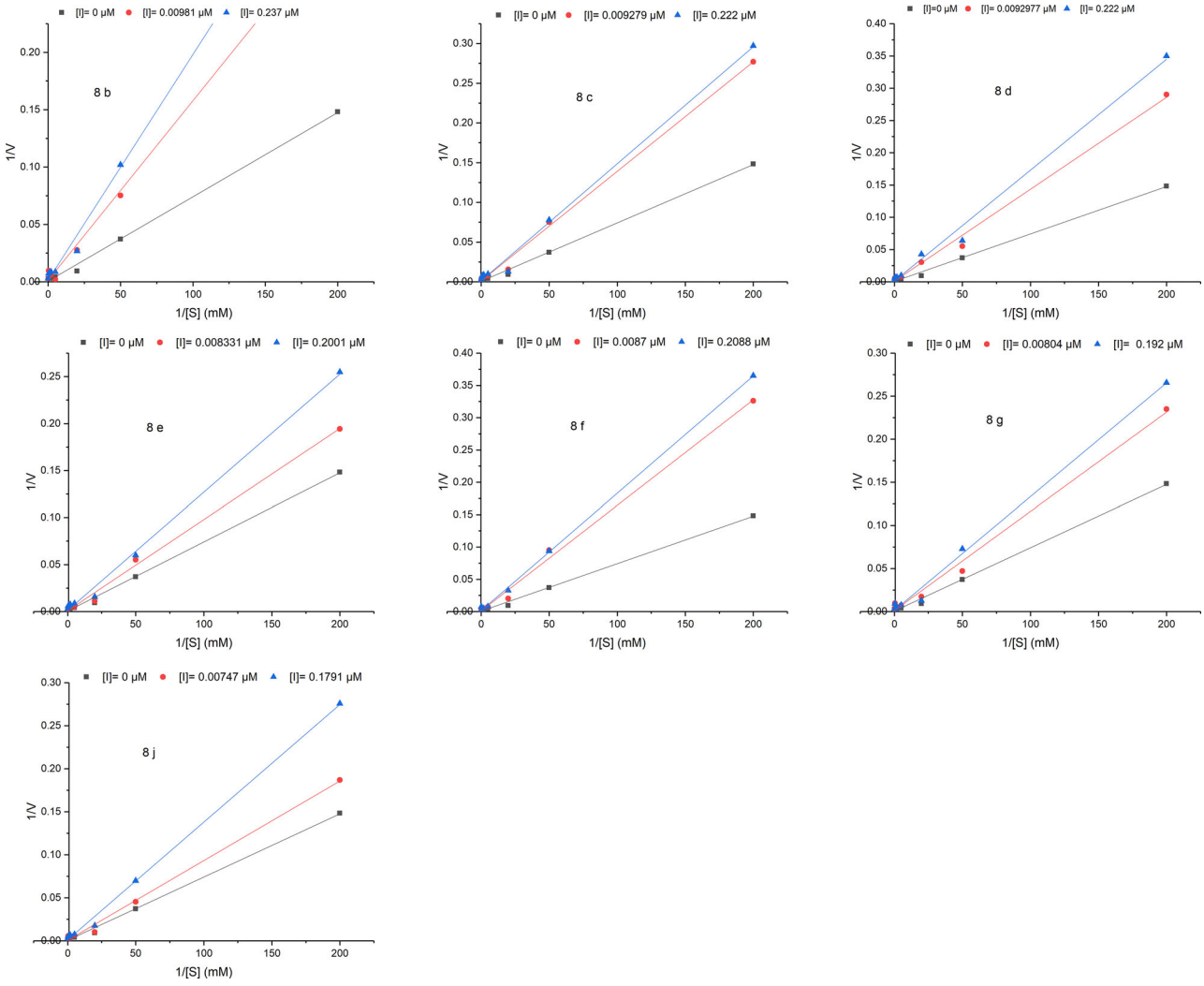

Figure 10. Lineweaver–Burk plots drawn to determine the inhibition types of **8b**, **8c**, **8d**, **8e**, **8f**, **8g** and **8j** molecules.

Inhibition studies

In enzyme inhibition studies, Gefitinib (Iressa) as reference molecule and synthesized molecules were used. A series of measurements were made for each molecule at different concentration ranges. With the results obtained, IC_{50} values were calculated by plotting the Relative Activity (%) graph against the inhibitor concentration for each organic molecule and Gefitinib (Supplementary Material Table S3). The inhibition type of synthesized organic molecules was determined from Lineweaver–Burk graphs, and K_i values were calculated mathematically (Supplementary Material Table S4, Figures 9 and 10). Molecules with the best IC_{50} value were selected and the type of inhibition caused by these molecules was investigated. In order to elucidate the inhibition mechanism, studies were carried out in the inhibitor concentration range that causes inhibition of 10–75% (Copeland, 2005). However, the solubility of organic molecules and the inhibition effect of the solvent were effective in determining the concentration range of organic molecules used in the study. Since the behavior of each of the organic molecules we evaluated in

the study was different, the concentration ranges of each molecule used in inhibition studies also differed (Figures 9 and 10). While **7c**, **7e** and **7g** molecules showed uncompetitive inhibition, other molecules caused noncompetitive inhibition. It has been reported in the literature that the inhibition mechanisms of compounds derived from a certain starting molecule and derivatized to variable groups at certain positions may be similar (Copeland, 2005). In the case of noncompetitive inhibition, inhibition occurs as a result of weak interaction and reversible binding to the free enzyme or enzyme–substrate complex outside the active site of the enzyme. Uncompetitive inhibition, on the other hand, occurs when the inhibitor binds to the enzyme substrate complex with weak interaction and reversible. In both cases, inhibition occurs outside the substrate binding site of the enzyme. As a result of these studies, the K_i value was calculated mathematically for the molecules whose inhibition type was investigated. From the results obtained, it is seen that the molecule with the best K_i value is **8g** compound with 0.00232 μM, followed by **7c** compound with 0.0889 μM. It was observed that the K_i values of the other compounds were almost close to each other (Supplementary Material Table S4). In the research conducted in the literature databases, it was seen that there was no study in which the IC_{50} values of inhibitor molecules were found using an ELISA kit from before 2018, regarding molecules with a 1,2,4-triazole skeleton. In addition, a study in which the detailed inhibition mechanism was investigated and K_i values were determined on the molecules with the skeleton we used in the study could not be found in the literature.

Conclusion

As a result of these kinetic studies carried out within the scope of the study, it is thought that a new perspective can be brought to the literature in terms of examining the inhibition effect of 1,2,4-trizaol compounds on hEGFR and determining the inhibition type. In addition, considering the findings obtained, it can be said that the IC_{50} values of the synthesized molecules **7c**, **8e**, **8g** and **8f** can be promising and developable inhibitor candidate molecules when compared to Gefitinib, which is used as a standard inhibitor. Considering the data obtained as a result of inhibition and kinetic studies, it is predicted that the way to design and synthesize more effective 1,2,4-triazole molecules, supported by docking studies and optimized biochemically, can be opened.

Disclosure statement

No potential conflict of interest was reported by the authors.

Funding

This work was financially supported by the Scientific and Technological Research Council of Turkey (TUBITAK) [Grant Number 118Z187].

ORCID

Senay Hamarat Sanlier http://orcid.org/0000-0001-6532-7221

References

Abou-Seri, S. M. (2010). Synthesis and biological evaluation of novel 2,4′-bis substituted diphenylamines as anticancer agents and potential epidermal growth factor receptor tyrosine kinase inhibitors. *European journal of Medicinal Chemistry*, *45*(9), 4113–4121. https://doi.org/10.1016/j.ejmech.2010.05.072

Akhtar, T., Hameed, S., Khan, K. M., Khan, A., & Choudhary, M. I. (2010). Design, synthesis, and urease inhibition studies of some 1,3,4-oxadiazoles and 1,2,4-triazoles derived from mandelic acid. *Journal of Enzyme İnhibition and Medicinal Chemistry*, *25*(4), 572–576. https://doi.org/10.3109/14756360903389864

Akin, S., Ayaloglu, H., Gultekin, E., Colak, A., Bekircan, O., & Akatin, M. Y. (2019). Synthesis of 1,2,4-triazole-5-on derivatives and determination of carbonic anhydrase II isoenzyme inhibition effects. *Bioorganic chemistry*, *83*, 170–179. https://doi.org/10.1016/j.bioorg.2018.10.042

Ali, A. A., Soliman, M. A., Aouad, M. R., Messali, M., & Rezki, N. (2019). Synthesis, characterization, and antimicrobial screening of novel 1,2,4-triazoles, 1,3,4-thiadiazoles, and 1,3,4-oxadiazoles bearing the ındole moiety. *Organic Preparations and Procedures International*, *51*(3), 270–286. https://doi.org/10.1080/00304948.2019.1599791

Ayati, A., Moghimi, S., Salarinejad, S., Safavi, M., Pouramiri, B., & Foroumadi, A. (2020). A review on progression of epidermal growth factor receptor (EGFR) inhibitors as an efficient approach in cancer targeted therapy. *Bioorganic chemistry*, *99*, 103811. https://doi.org/10.1016/j.bioorg.2020.103811

Bekircan, O., Danış, Ö., Şahin, M. E., & Çetin, M. (2022). Monoamine oxidase A and B inhibitory activities of 3,5-diphenyl-1,2,4-triazole substituted [1,2,4]triazolo[3,4-b][1,3,4]thiadiazole derivatives. *Bioorganic Chemistry*, *118*, 105493. https://doi.org/10.1016/j.bioorg.2021.105493

Bekircan, O., Ülker, S., & Menteşe, E. (2015). Synthesis of some novel heterocylic compounds derived from 2-[3-(4-chlorophenyl)-5-(4-methoxybenzyl)-4H-1,2,4-triazol-4-yl]acetohydrazide and investigation of their lipase and α-glucosidase inhibition. *Journal of Enzyme İnhibition and Medicinal Chemistry*, *30*(6), 1002–1009. https://doi.org/10.3109/14756366.2014.1003213

Bhatia, P., Sharma, V., Alam, O., Manaithiya, A., Alam, P., Alam, M. T., Imran., & M., Kahksha. (2020). Novel quinazoline-based EGFR kinase inhibitors: A review focussing on SAR and molecular docking studies. *European journal of Medicinal Chemistry*, *204*, 112640., https://doi.org/10.1016/j.ejmech.2020.112640

Brueggemeier, R. W., Hackett, J. C., & Diaz-Cruz, E. S. (2005). Aromatase inhibitors in the treatment of breast cancer. *Endocrine reviews*, *26*(3), 331–345. https://doi.org/10.1210/er.2004-0015

Channar, P. A., Saeed, A., Larik, F. A., Rashid, S., Iqbal, Q., Rozi, M., Younis, S., & Mahar, J. (2017). Design and synthesis of 2,6-di(substituted phenyl)thiazolo[3,2-b]-1,2,4-triazoles as α-glucosidase and α-amylase inhibitors, co-relative pharmacokinetics and 3D QSAR and risk analysis. *Biomedicine & Pharmacotherapy = Biomedecine & Pharmacotherapie*, *94*, 499–513. https://doi.org/10.1016/j.biopha.2017.07.139

Cohen, S. (1962). Isolation of a mouse submaxillary gland protein accelerating ıncisor eruption and eyelid opening in the new-born animal. *The Journal of Biological Chemistry*, *237*(5), 1555–1562. https://doi.org/10.1016/S0021-9258(19)83739-0

Copeland, R. A. (2005). Evaluation of enzyme inhibitors in drug discovery. A guide for medicinal chemists and pharmacologists. *Methods of Biochemical Analysis*, *46*, 1–265. https://doi.org/10.1016/j.drudis.2006.06.017.

El-Sherief, H. A. M., Youssif, B. G., Abbas Bukhari, S. N., Abdelazeem, A. H., Abdel-Aziz, M., & Abdel-Rahman, H. M. (2018). Synthesis, anticancer activity and molecular modeling studies of 1,2,4-triazole derivatives as EGFR inhibitors. *European journal of Medicinal Chemistry*, *156*, 774–789. https://doi.org/10.1016/j.ejmech.2018.07.024

El-Sherief, H. A. M., Youssif, B. G. M., Bukhari, S. N. A., Abdel-Aziz, M., & Abdel-Rahman, H. M. (2018). Novel 1,2,4-triazole derivatives as potential anticancer agents: Design, synthesis, molecular docking and mechanistic studies. *Bioorganic chemistry*, *76*, 314–325. https://doi.org/10.1016/j.bioorg.2017.12.013

El-Wahab, H. A. A. A., Ali, A. M., Abdel-Rahman, H. M., & Qayed, W. S. (2021). Synthesis, biological evaluation, and molecular modeling studies of acetophenones-tethered 1,2,4-triazoles and their oximes as epidermal growth factor receptor inhibitors. *Chemical Biology & Drug Design*, *00*, 1–13. https://doi.org/10.1111/cbdd.13982

Francis, J. E., Gorczyca, L. A., Mazzenga, G. C., & Meckler, H. (1987). A convenient synthesis of 3,5-disubstituted-1,2,4-triazoles. *Tetrahedron Letters*, *28*(43), 5133–5136. https://doi.org/10.1016/S0040-4039(00)95610-7

Gajanan Khanage, S., Raju, A., Baban Mohite, P., & Bhanudas Pandhare, R. (2013). Analgesic activity of some 1,2,4-triazole heterocycles clubbed with pyrazole, tetrazole, isoxazole and pyrimidine. *Advanced Pharmacetual Bulletin*, *3*(1), 13–18. https://doi.org/10.5681/apb.2013.003

Gao, F., Wang, T., Xiao, J., & Huang, G. (2019). Antibacterial activity study of 1,2,4-triazole derivatives. *European journal of Medicinal Chemistry*, *173*, 274–281. https://doi.org/10.1016/j.ejmech.2019.04.043

Gomaa, H. A. M., El-Sherief, H. A. M., Hussein, S., Gouda, A. M., Salem, O. I. A., Alharbi, K. S., Hayallah, A. M., & Youssif, B. G. M. (2020). Novel 1,2,4-triazole derivatives as apoptotic inducers targeting p53: Synthesis and antiproliferative activity. *Bioorganic chemistry*, *105*, 104369. https://doi.org/10.1016/j.bioorg.2020.104369

Grytsai, O., Valiashko, O., Penco-Campillo, M., Dufies, M., Hagege, A., Demange, L., Martial, S., Pagès, G., Ronco, C., & Benhida, R. (2020). Synthesis and biological evaluation of 3-amino-1,2,4-triazole derivatives as potential anticancer compounds. *Bioorganic chemistry*, *104*, 104271. https://doi.org/10.1016/j.bioorg.2020.104271

Gultekin, E., Bekircan, O., Kolcuoğlu, Y., & Akdemir, A. (2021). Synthesis of new 1,2,4-triazole-(thio)semicarbazide hybrid molecules: Their tyrosinase inhibitor activities and molecular docking analysis. *Archiv der Pharmazie*, *354*(8), 2100058. https://doi.org/10.1002/ardp.202100058

Inturi, S. B., Kalita, B., & Ahamed, A. J. (2016). I2 mediated one-pot synthesis of 1,2,4-triazoles from amidines and imidates. *Tetrahedron Letters*, *57*(21), 2227–2230. https://doi.org/10.1016/j.tetlet.2016.04.015

Kang, B.-R., Shan, A.-L., Li, Y.-P., Xu, J., Lu, S.-M., & Zhang, S.-Q. (2013). Discovery of 2-aryl-8-hydroxy (or methoxy)-isoquinolin-1(2H)-ones as novel EGFR inhibitor by scaffold hopping. *Bioorganic & Medicinal Chemistry*, *21*(22), 6956–6964. https://doi.org/10.1016/j.bmc.2013.09.027

Khan, I., Ali, S., Hameed, S., Rama, N. H., Hussain, M. T., Wadood, A., Uddin, R., Ul-Haq, Z., Khan, A., Ali, S., & Iqbal Choudhary, M. (2010). Synthesis, antioxidant activities and urease inhibition of some new 1,2,4-triazole and 1,3,4-thiadiazole derivatives. *European journal of Medicinal Chemistry*, *45*(11), 5200–5207. https://doi.org/10.1016/j.ejmech.2010.08.034

Kharb, R., Shahar Yar, M., & Chander Sharma, P. (2011). Recent advances and future perspectives of triazole analogs as promising antiviral agents. *Mini reviews in Medicinal Chemistry*, *11*(1), 84–96. https://doi.org/10.2174/138955711793564051

Konetzki, I., Bouyssou, T., Hoenke, C., & Schnapp, A. (2006). New long-acting betamimetics for the treatment of respiratory diseases. Germany patent DE102005007654 A1 2006-08-24.

Küçükgüzel, Ş. G., & Çıkla-Süzgün, P. (2015). Recent advances bioactive 1,2,4-triazole-3-thiones. *European journal of Medicinal Chemistry*, *97*, 830–870. https://doi.org/10.1016/j.ejmech.2014.11.033

Küçükgüzel, İ., Tatar, E., Küçükgüzel, Ş. G., Rollas, S., & De Clercq, E. (2008). Synthesis of some novel thiourea derivatives obtained from 5-[(4-aminophenoxy)methyl]-4-alkyl/aryl-2,4-dihydro-3H-1,2,4-triazole-3-thiones and evaluation as antiviral/anti-HIV and anti-tuberculosis agents. *European journal of Medicinal Chemistry*, *43*(2), 381–392. https://doi.org/10.1016/j.ejmech.2007.04.010

Kumar, A., & Chauhan, S. (2021). Pancreatic lipase inhibitors: The road voyaged and successes. *Life Sciences*, *271*, 119115. https://doi.org/10.1016/j.lfs.2021.119115

Labute, P. (2008). The generalized Born/volume integral implicit solvent model: Estimation of the free energy of hydration using London dispersion instead of atomic surface area. *Journal of Computational Chemistry*, *29*(10), 1693–1698. https://doi.org/10.1002/jcc.20933

Legru, A., Verdirosa, F., Hernandez, J.-F., Tassone, G., Sannio, F., Benvenuti, M., Conde, P.-A., Bossis, G., Thomas, C. A., Crowder, M. W., Dillenberger, M., Becker, K., Pozzi, C., Mangani, S., Docquier, J.-D., & Gavara, L. (2021). 1,2,4-Triazole-3-thione compounds with a 4-ethyl alkyl/aryl sulfide substituent are broad-spectrum metallo-β-lactamase inhibitors with re-sensitization activity. *European journal of Medicinal Chemistry*, *226*, 113873. https://doi.org/10.1016/j.ejmech.2021.113873

Li, M., Xue, N., Liu, X., Wang, Q., Yan, H., Liu, Y., Wang, L., Shi, X., Cao, D., Zhang, K., & Zhang, Y. (2021). Discovery of potent EGFR ınhibitors with 6-arylureido-4-anilinoquinazoline derivatives. *Frontiers in Pharmacology*, *12*, 1254. https://doi.org/10.3389/fphar.2021.647591

Lineweaver, H., & Burk, D. (1934). The determination of enzyme dissociation constants. *Journal of the American Chemical Society*, *56*(3), 658–666. https://doi.org/10.1021/ja01318a036

Lü, S., Zheng, W., Ji, L., Luo, Q., Hao, X., Li, X., & Wang, F. (2013). Synthesis, characterization, screening and docking analysis of 4-anilinoquinazoline derivatives as tyrosine kinase inhibitors. *European journal of Medicinal Chemistry*, *61*, 84–94. https://doi.org/10.1016/j.ejmech.2012.07.036

Ma, Y. C., Wang, Z. X., Jin, S. J., Zhang, Y. X., Hu, G. Q., Cui, D. T., Wang, J. S., Wang, M., Wang, F. Q., & Zhao, Z. J. (2016). Dual ınhibition of topoisomerase II and tyrosine kinases by the novel bis-fluoroquinolone chalcone-like derivative HMNE3 in human pancreatic cancer cells. *PloS one*, *11*(10), e0162821. https://doi.org/10.1371/journal.pone.0162821

Mohamed, M. A. A., Abd Allah, O. A., Bekhit, A. A., Kadry, A. M., & El-Saghier, A. M. M. (2020). Synthesis and antidiabetic activity of novel triazole derivatives containing amino acids. *Journal of Heterocyclic Chemistry*, *57*(6), 2365–2378. https://doi.org/10.1002/jhet.3951

Mohassab, A. M., Hassan, H. A., Abdelhamid, D., Gouda, A. M., Youssif, B. G. M., Tateishi, H., Fujita, M., Otsuka, M., & Abdel-Aziz, M. (2021). Design and synthesis of novel quinoline/chalcone/1,2,4-triazole hybrids as potent antiproliferative agent targeting EGFR and $BRAF^{V600E}$ kinases. *Bioorganic chemistry*, *106*, 104510. https://doi.org/10.1016/j.bioorg.2020.104510

Mokhtar, A. M., El-Messery, S. M., Ghaly, M. A., & Hassan, G. S. (2020). Targeting EGFR tyrosine kinase: Synthesis, in vitro antitumor evaluation, and molecular modeling studies of benzothiazole-based derivatives. *Bioorganic chemistry*, *104*(104259), 104259. https://doi.org/10.1016/j.bioorg.2020.104259

Normanno, N., Bianco, C., De Luca, A., Maiello, M. R., & Salomon, D. S. (2003). Target-based agents against ErbB receptors and their ligands: A novel approach to cancer treatment. *Endocrine-Related Cancer*, *10*(1), 1–21. https://doi.org/10.1677/erc.0.0100001

Olayioye, M. A., Neve, R. M., Lane, H. A., & Hynes, N. E. (2000). The ErbB signaling network: Receptor heterodimerization in development and cancer. *The EMBO Journal*, *19*(13), 3159–3167. https://doi.org/10.1093/emboj/19.13.3159

Olgen, S., Isgör, Y. G., & Coban, T. (2008). Synthesis and activity of novel 5-substituted pyrrolo[2,3-d]pyrimidine analogues as pp60(c-Src) tyrosine kinase inhibitors. *Archiv der Pharmazie*, *341*(2), 113–120. https://doi.org/10.1002/ardp.200700141

Plech, T., Kaproń, B., Łuszczki, J. J., Wujec, M., Paneth, A., Siwek, A., Kołaczkowski, M., Żołnierek, M., & Nowak, G. (2014). Studies on the anticonvulsant activity and ınfluence on GABA-ergic neurotransmission of 1,2,4-triazole-3-thione- based compounds. *Molecules*, *19*(8), 11279–11299. https://doi.org/10.3390/molecules190811279

Saravolatz, L. D., Johnson, L. B., & Kauffman, C. A. (2003). Voriconazole: A new triazole antifungal agent. *Clinical infectious Diseases*, *36*(5), 630–637. https://doi.org/10.1086/367933

Shaker, R. M. (2006). The chemistry of mercapto- and thione- substituted 1,2,4-triazoles and their utility in heterocyclic synthesis. *ARKIVOC*, *2006*(9), 59–112.

Spira, A., & Ettinger, D. S. (2004). Multidisciplinary management of lung cancer. *The New England Journal of Medicine*, *350*(4), 379–392. https://doi.org/10.1056/NEJMra035536

Sudhakar, A. (2009). History of cancer, ancient and modern treatment methods. *Journal of Cancer Science & Therapy*, *1*(2), 1–4.https://doi.org/10.4172/1948-5956.100000e2

Tariq, S., Kamboj, P., Alam, O., & Amir, M. (2018). 1,2,4-Triazole-based benzothiazole/benzoxazole derivatives: Design, synthesis, p38α MAP kinase inhibition, anti-inflammatory activity and molecular docking studies. *Bioorganic Chemistry*, *81*, 630–641. https://doi.org/10.1016/j.bioorg.2018.09.015

Varkondi, E., Schäfer, E., Bökönyi, G., Gyökeres, T., Orfi, L., Petak, I., Pap, A., Szokoloczi, O., Keri, G., & Schwab, R. (2005). Comparison of ELISA-based tyrosine kinase assays for screening EGFR inhibitors. *Journal of Receptor and Signal Transduction Research*, *25*(1), 45–56. https://doi.org/10.1081/RRS-200055095

Vats, L., Kumar, R., Bua, S., Nocentini, A., Gratteri, P., Supuran, C. T., & Sharma, P. K. (2019). Continued exploration and tail approach synthesis of benzenesulfonamides containing triazole and dual triazole moieties as carbonic anhydrase I, II, IV and IX inhibitors. *European Journal of Medicinal Chemistry*, *183*(111698), 111698. https://doi.org/10.1016/j.ejmech.2019.111698

Wei, H., Duan, Y., Gou, W., Cui, J., Ning, H., Li, D., Qin, Y., Liu, Q., & Li, Y. (2019). Design, synthesis and biological evaluation of novel 4-anilinoquinazoline derivatives as hypoxia-selective EGFR and VEGFR-2 dual inhibitors. *European journal of Medicinal Chemistry*, *181*(111552), 111552. https://doi.org/10.1016/j.ejmech.2019.07.055

Xia, J., Huang, X., & Cai, M. (2019). Heterogeneous copper(I)-catalyzed cascade addition–oxidative cyclization of nitriles with 2-aminopyridines or amidines: Efficient and practical synthesis of 1,2,4-triazoles. *Synthesis*, *51*(09), 2014–2022.

Yang, H., Yan, R., Jiang, Y., Yang, Z., Zhang, X., Zhou, M., Wu, X., Zhang, T., & Zhang, J. (2020). Design, synthesis and biological evaluation of 2-amino-4-(1,2,4-triazol)pyridine derivatives as potent EGFR inhibitors to overcome TKI-resistance. *European journal of Medicinal Chemistry*, *187*(111966), 111966. https://doi.org/10.1016/j.ejmech.2019.111966

Yılmaz, F., & Mentese, E. (2014). A rapid protocol for the synthesis of N-[2-(alkyl/aryl)-4-phenyl-1Himidazol- 1-yl] benzamides via microwave technique. *Current Microwave Chemistry*, *1*(1), 47–51. https://doi.org/10.2174/2213335601999140221111915

Zhang, J., Yang, P. L., & Gray, N. S. (2009). Targeting cancer with small molecule kinase inhibitors. *Nature reviews. Cancer*, *9*(1), 28–39. https://doi.org/10.1038/nrc2559